

APPENDIX **A**

Review of Metallic Structure

THE WORD *METAL*, derived from the Greek *metallon*, is believed to have originated as a verb meaning to seek, search after, or inquire about. Today, a metal is defined as any element that tends to lose electrons from the outer shells of its atoms. The resulting positive ions are held together in crystalline structure by the cloud of these free electrons in what is known as the metallic bond. The metallic bond yields three physical characteristics typical of solid metals: (1) metals are good conductors of electricity, (2) metals are good conductors of heat, and (3) metals have a lustrous appearance. In addition, most metals are malleable, ductile, and generally denser than other elemental substances. Those elements that do not display the characteristics of the metallic elements are called nonmetals. However, there are some elements that behave as metals under some circumstances and as nonmetals under different circumstances. These are now called semimetals, but have also been called metalloids, meaning like metals. The boundaries separating the regions in the periodic table covered by the different classes of elements are not distinct, except that nonmetals never form positive ions. A simplified periodic table is shown in Fig. A.1, highlighting the elements that are currently considered to be metals.

A.1 Periodic Table

In the periodic table, it is the number of electrons in the outer shell that affects the properties of the elements the most. Those elements that have the same number of electrons in their outermost electron shells, and therefore have similar chemical behavior, are placed in columns. For example, lithium, sodium, and potassium each have a single electron in their outer shells and are chemically very similar. They all oxidize very rapidly and react vigorously with water, liberating hydrogen and forming soluble hydroxides. They are physically very similar, being soft light metals with

Metals										Nonmetals							
I A	II A	III A	IV A	V A	VI A	VII A	VIII B					I B	II B	0			
1 H	2 He																
3 Li	4 Be										5 B	6 C	7 N	8 O	9 F	10 Ne	
11 Na	12 Mg										13 Al	14 Si	15 P	16 S	17 Cl	18 Ar	
19 K	20 Ca	21 Sc	22 Ti	23 V	24 Cr	25 Mn	26 Fe	27 Co	28 Ni	29 Cu	30 Zn	31 Ga	32 Ge	33 As	34 Se	35 Br	36 Kr
37 Rb	38 Sr	39 Y	40 Zr	41 Nb	42 Mo	43 Tc	44 Ru	45 Rh	46 Pd	47 Ag	48 Cd	49 In	50 Sn	51 Sb	52 Te	53 I	54 Xe
55 Cs	56 Ba	57 La	72 Hf	73 Ta	74 W	75 Re	76 Os	77 Ir	78 Pt	79 Au	80 Hg	81 Tl	82 Pb	83 Bi	84 Po	85 At	86 Rn
87 Fr	88 Ra	89 Ac	Lanthanide series														
			58 Ce	59 Pr	60 Nd	61 Pm	62 Sm	63 Eu	64 Gd	65 Tb	66 Dy	67 Ho	68 Er	69 Tm	70 Yb	71 Lu	
			Actinide series														
			90 Th	91 Pa	92 U	93 Np	94 Pu	95 Am	96 Cm	97 Bk	98 Cf	99 Es	100 Fm	101 Md	102 No	103 Lw	

Fig. A.1 Periodic table of the elements. Source: Ref A.1

a somewhat silver color. At the other end of the periodic table, the gases fluorine and chlorine, with seven electrons in their outer shells, also have similar chemical properties. Both are gases with strong nonmetallic properties. At the far right side of the periodic table, the noble gases helium, neon, and argon all contain eight electrons in their outer shells. Because this fills the shell, these gases are nonreactive, or inert, under normal circumstances. Therefore, the chemical interaction between elements is governed by the number of electrons present in the outer shell. When the outer shell is filled, the atom has no further tendency to combine or react with other atoms.

Metallic properties depend on both the nature of their constituent atoms and the way in which they are assembled. Assemblies of atoms can be gases, liquids, or solids. When they are in the solid state, metals are normally arranged in a crystalline structure. The crystalline nature of metals is responsible for their ultimate engineering usefulness, and the crystalline arrangement strongly influences their processing. Although metals can exist as single crystals, they are more commonly polycrystalline solids with crystalline grains of repeating atomic packing sequences. Periodic crystalline order is the equilibrium structure of all solid metals. Crystalline structures are a dominant factor in determining mechanical properties, and crystal structures also play an important role in the magnetic, electri-

cal, and thermal properties. The greatest bonding energy occurs when the atoms are closely packed, and the atoms in a crystalline structure tend to pack as densely as possible. In addition, total metallic bonding energy is increased when each atom has the greatest possible number of nearest-neighbor atoms. However, due to a shared bonding arrangement in some metals that is partially metallic and partially covalent, some metals do not crystallize into these close-packed structures. Covalent tendencies appear as one moves closer to the nonmetals on the periodic table. As one moves rightward across the periodic table, progressively greater numbers of metals have looser-packed structures. Most metals bordering the nonmetals possess more complex structures with lower packing densities, because covalent bonding plays a large role in determining their crystal structures. The directionality of covalent bonding dictates fewer nearest neighbors than exist in densely packed metallic crystals. For metals near the nonmetals on the right side of the periodic table, where electronegativities are high, covalency becomes a major part of the bonding.

Properties important to the engineer are strongly influenced by crystal structure. One of the most important properties related to crystal structure is ductility. Densely packed structures usually allow motion on one or more slip planes, permitting the metal to deform plastically without fracturing. Ductility is vital for easy formability and for fracture toughness, two properties that give metals a great advantage over ceramic materials for many engineering uses.

A.2 Bonding in Solids

Bonding in solids may be classified as either primary or secondary bonding. Methods of primary bonding include the metallic, ionic, and covalent bonds. Secondary bonds are much weaker bonding mechanisms that are only predominant when one of the primary bonding mechanisms is absent. When two atoms are brought close to each other, there will be a repulsion between the negatively charged electrons of each atom. The repulsion force increases rapidly as the distance of separation decreases. However, when the separation is large, there is attraction between the positive nucleus charge and the negative charge of the electrons. At some equilibrium distance, the attractive and repulsive forces balance each other and the net force is zero. At this equilibrium distance, the potential energy is at a minimum, as shown in Fig. A.2. The magnitude of this energy is known as the bond energy, usually expressed in kJ/mol. Primary bond energies range from 100 to 1,000 kJ/mol, while the much weaker secondary bonds are on the order of only 1 to 60 kJ/mol. The equilibrium distance, a_0 , is the bond length. Strong primary bonds have large forces of attraction with bond lengths of 1 to 2 Å, while the weaker secondary bonds have larger bond lengths of 2 to 5 Å. While it is convenient to discuss the four major types of bonding separately, it should be recognized that although metal-

lic bonding may be predominate, other types of bonding, in particular covalent bonding, may also be present. A comparison of the some of the properties of the different bond types is given in Table A.1.

Metallic bonding occurs when each of the atoms of the metal contributes its valence electrons to the formation of an electron cloud that surrounds the positively charged metal ions, as illustrated in Fig. A.3. Hence, the valence electrons are shared by all of the atoms. In this bond, the positively charged ions repel each other uniformly, so they arrange themselves into a regular pattern that is held together by the negatively charged electron cloud. Because the negative electron cloud surrounds each of the positive ions that make up the orderly three-dimensional crystal structure, strong electronic attraction holds the metal together. A characteristic of metallic bonding is the fact that every positive ion is equivalent. Ideally, a

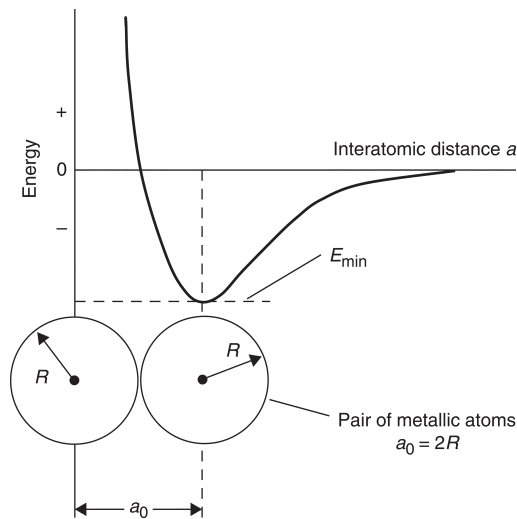


Fig. A.2 Bond energy in metallic bond. Source: Ref A.1

Table A.1 General characteristics of bond types

Properties	Metallic bond	Covalent bond	Ionic bond	Secondary bonds
Examples	Copper, nickel, iron	Diamond, carborundum	NaCl, CaCl ₂	Wax, argon
Mechanical	Weaker than ionic or covalent bond. Tough and ductile. Nondirectional	Very hard and brittle. Fails by cleavage. Strongly directional	Hardness increases with ionic charge. Fails by cleavage. Nondirectional	Weak and soft. Can be plastically deformed
Thermal	Moderately high melting points. Good conductors of heat	Very high melting points. Thermal insulators	Fairly high melting points. Thermal insulators	Low melting points
Electrical	Conductors	Insulators	Insulators	Insulators
Optical	Opaque and reflecting	Transparent or opaque. High refractive index	Transparent. Colored by ions	Transparent

Source: Ref A.1 as published in Ref A.2

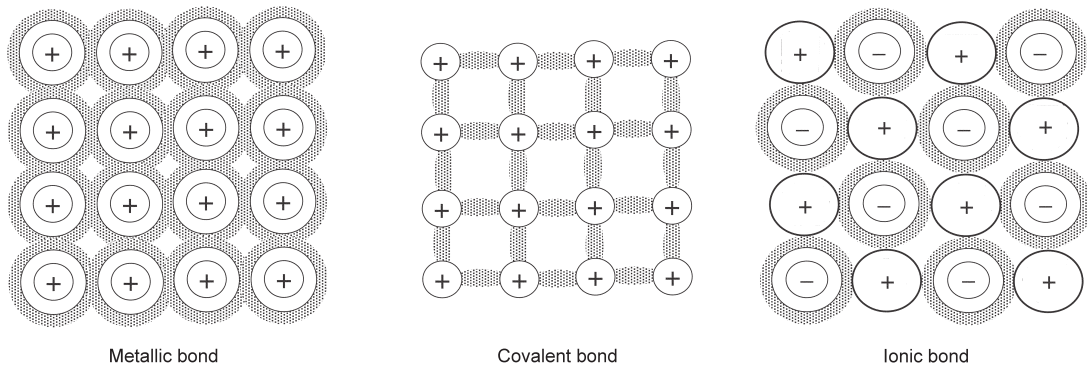


Fig. A.3 Primary bonding mechanisms. Source: Ref A.1

symmetrical ion is produced when a valence electron is removed from the metal atom. As a result of this ion symmetry, metals tend to form highly symmetrical, close-packed crystal structures. They also have a large number of nearest-neighboring atoms (usually 8 to 12), which helps to explain their high densities and high elastic stiffness.

Because the valence electrons are no longer attached to specific positive ions and they are free to travel among the positive ions, metals exhibit high electrical and thermal conductivity. The opaque luster of metals is due to the reflection of light by the free electrons. A light wave striking the surface causes the free electrons to vibrate and absorb all the energy of the wave and prevent transmission. The vibrating electrons then re-emit, or reflect, the wave from the surface. The ability of metals to undergo significant amounts of plastic deformation is also due to the metallic bond. Under the action of an applied shearing force, layers of the positive ion cores can slide over each other and re-establish their bonds without drastically altering their relationship with the electron cloud. The ability to alloy, or mix several metals together in the liquid state, is one of the keys to the flexibility of metals. In the liquid state, solubility is often complete, while in the solid state, solubility is generally much more restricted. This change in solubility with temperature forms the basis for heat treatments that can vary the strength and ductility over quite wide ranges.

In general, the fewer the valence electrons and more loosely they are held, the more metallic is the bonding. Metals such as copper and silver, which have few valence electrons, are very good conductors of electricity and heat, because their few valence electrons are highly mobile. As the number of valence electrons increases and the tightness with which they are held to the nucleus increases, the valence electrons become localized and the bond becomes more covalent. The transition metals, such as iron and nickel, have incomplete *d*-shells and exhibit some covalent bonding, which helps explain their relatively high melting points. Tin is interest-

ing in that it has two crystalline forms, one that is mostly metallic and ductile and another that is mostly covalent and very brittle. Intermetallic compounds can also be formed between two metals in which the bonding is partly metallic and partly ionic. As the electronegativity difference between the two metals increases, the bonding becomes more ionic in nature. For example, aluminum and vanadium both have an electronegativity of 1.5 and the difference is 0, so the compound Al_3V is primarily metallic. On the other hand, aluminum and lithium (electronegativity of 1.0) have an electronegativity difference of 0.5; thus, when they form the compound AlLi , the bond is a combination of metallic and ionic.

Ionic bonding, also shown in Fig. A.3, is a result of electrical attraction between alternately placed positive and negative ions. In the ionic bond, the electrons are shared by an electropositive ion (cation) and an electronegative ion (anion). The electropositive ion gives up its valence electrons, while the electronegative ion captures them to produce ions having full electron orbitals or suborbitals. As a consequence, there are no free electrons available to conduct electricity. In ionically bonded solids such as salts, there are very few slip systems along which atoms can move. This is a consequence of the electrically charged nature of the ions. For slip in some directions, ions of like charge must be brought into close proximity to each other, and because of electrostatic repulsion, this mode of slip is very restricted. This is not a problem in metals, because all atoms are electronically neutral. No electrical conduction of the kind found in metals is possible in ionic crystals, but weak ionic conduction occurs as a result of the motion of the individual ions. When subjected to stresses, ionic crystals tend to cleave, or break, along certain planes of atoms rather than deform in a ductile fashion as metals do.

Ionic bonds form between electropositive metals and electronegative nonmetals. The further apart the two are on the periodic table, the more likely they are to form ionic bonds. For example, sodium (Na) is on the far left side of the periodic table in Group I, while chlorine (Cl) is on the far left side in Group VII. Sodium and chlorine combine to form common table salt (NaCl). As shown in Fig. A.4, the sodium atom gives up its outer valence electron, which is transferred to the outer electron shell of the chlorine atom. Because the outer shell of chlorine now contains eight electrons, similar to the noble gases, it is an extremely stable configuration. In terms of symbols, the sodium ion is written as Na^+ , and the chlorine ion is written as Cl^- . When the two combine to form an ionic bond, the compound (NaCl) is neutral because the charges balance. Because the positively charged cation can attract multiple negatively charged anions, the ionic bond is nondirectional.

Covalent Bonding. Many elements that have three or more valence electrons are bound into crystal structures by forces arising from the

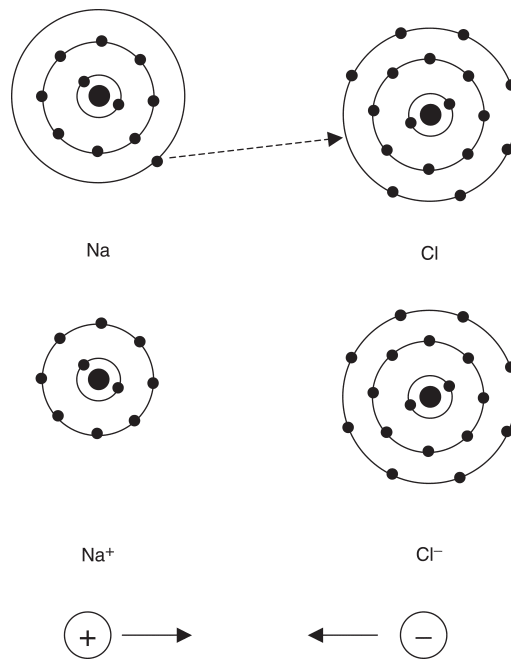


Fig. A.4 Ionic bonding in NaCl. Source: Ref A.1

sharing of electrons. The nature of this covalent bonding is shown schematically in Fig. A.3. To complete the octet of electrons needed for atomic stability, electrons must be shared with $8-N$ neighboring atoms, where N is the number of valence electrons in the given element. High hardness and low electrical conductivity are general characteristics of solids of this type. In covalently bonded ceramics, the bonding between atoms is specific and directional, involving the exchange of electron charge between pairs of atoms. Thus, when covalent crystals are stressed to a sufficient extent, they exhibit brittle fracture due to a separation of electron pair bonds, without subsequent reformation. It should also be noted that ceramics are rarely either all ionically or covalently bonded; they usually consist of a mix of the two types of bonds. For example, silicon nitride (Si_3N_4) consists of approximately 70% covalent bonds and 30% ionic bonds.

Covalent bonds also form between electropositive elements and electronegative elements. However, the separation on the periodic table is not great enough to result in electron transfer as in the ionic bond. Instead, the valence electrons are shared between the two elements. For example, a molecule of methane (CH_4), shown in Fig. A.5, is held together by covalent bonds. Note that hydrogen, in Group I on the periodic table, and carbon in Group IV, are much closer together than sodium and chlorine that form ionic bonds. In a molecule of methane gas, four hydrogen atoms are combined with one carbon atom. The carbon atom has four electrons in its

outer shell, and these are combined with four more electrons, one from each of the four hydrogen atoms, to give a completed stable outer shell of eight electrons held together by covalent bonds. Each shared electron passes from an orbital controlled by one nucleus into an orbital shared by two nuclei. Covalent bonds, because they do not ionize, will not conduct electricity and are nonconductors. Covalent bonds form the basis for many organic compounds, including long-chain polymer molecules. As the molecule size increases, the bond strength of the material also increases. Likewise, the strength of long-chain molecules also increases with increases in chain length.

Secondary Bonding. Secondary, or van der Waals, bonding is weak in comparison to the primary metallic, ionic, and covalent bonds. Bond energies are typically on the order of only 10 kJ/mol (0.1 eV/atom). Although secondary bonding exists between virtually all atoms or molecules, its presence is usually obscured if any of the three primary bonding types is present. While van der Waals forces only play a minor role in metals, they are an important source of bonding for the inert gases that have stable electron structures, some molecular compounds such as water, and thermoplastic polymers where the main chains are covalently bonded but are held to other main chains by secondary bonding. Van der Waals bonding between two dipoles is illustrated in Fig. A.6.

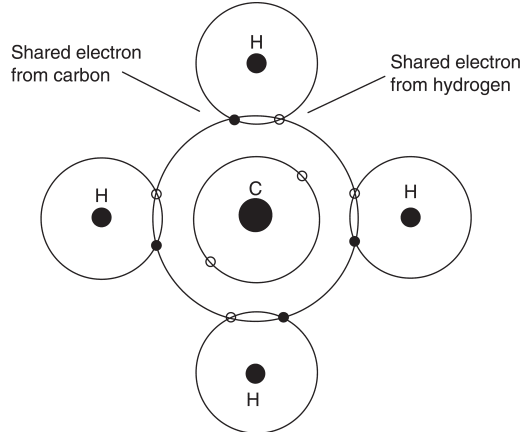


Fig. A.5 Covalent bonding in methane. Source: Ref A.1

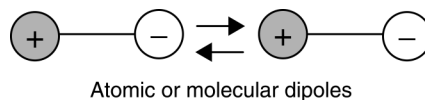


Fig. A.6 Van der Waals bonding between two dipoles. Source: Ref A.1

A.3 Crystalline Structure

When a substance freezes on cooling from the liquid state, it forms a solid that is either an amorphous or a crystalline structure. An amorphous structure is essentially a random structure. Although there may be what is known as short-range order, in which small groups of atoms are arranged in an orderly manner, it does not contain long-range order, in which all of the atoms are arranged in an orderly manner. Typical amorphous materials include glasses and almost all organic compounds. However, metals, under normal freezing conditions, normally form long-range, orderly crystalline structures. Except for glasses, almost all ceramic materials also form crystalline structures. Therefore, metals and ceramics are, in general, crystalline, while glasses and polymers are mostly amorphous.

Space Lattices and Crystal Systems. A crystalline structure consists of atoms, or molecules, arranged in a pattern that is repetitive in three dimensions. The arrangement of the atoms or molecules in the interior of a crystal is called its crystalline structure. A distribution of points (or atoms) in three dimensions is said to form a space lattice if every point has identical surroundings, as shown in Fig. A.7. The intersections of the lines, called lattice points, represent locations in space with the same kind of atom or group of atoms of identical composition, arrangement, and orientation. The geometry of a space lattice is completely specified by the lattice constants a , b , and c and the interaxial angles α , β , and γ . The unit cell of a crystal is the smallest pattern of arrangement that can be contained in a parallelepiped, the edges of which form the a , b , and c axes of the crystal.

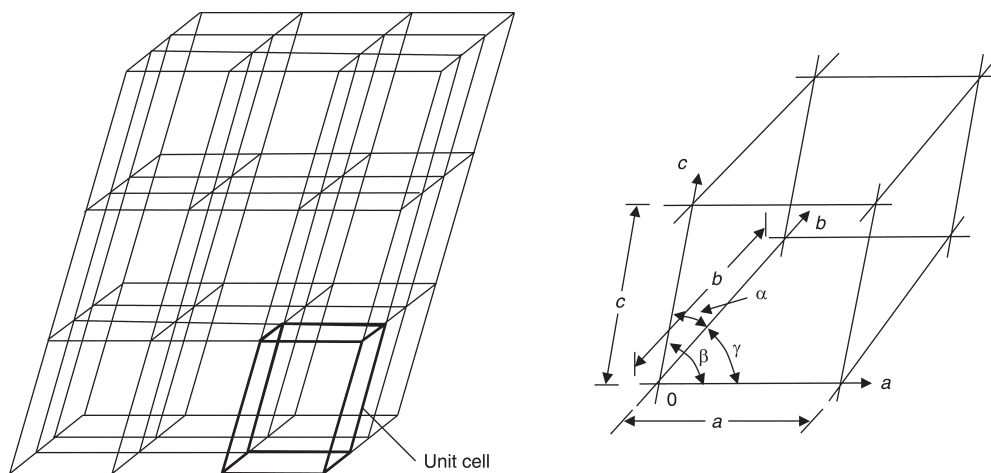


Fig. A.7 Space lattice and unit cell. Source: Ref A.1

When discussing crystal structure, it is usually assumed that the space lattice continues to infinity in all directions. In terms of a typical crystal (or grain) of, for example, iron that is 0.2 cm^3 in size, this may appear to be a preposterous assumption, but when it is realized that there are 10^{18} iron atoms in such a grain, the approximation to infinity seems much more plausible.

All crystal systems can be grouped into one of seven basic systems, as defined in Table A.2, which can be arranged in 14 different ways, called Bravais lattices, as shown in Fig. A.8. Almost all structural metals crystallize into one of three crystalline patterns: face-centered cubic (fcc), hexagonal close-packed (hcp), or body-centered cubic (bcc), illustrated in Fig. A.9. It should be noted that the unit cell edge lengths and axial angles are unique for each crystalline substance. The unique edge lengths are called lattice parameters. Axial angles other than 90° or 120° can also change slightly with changes in composition. When the edges of the unit cell are not equal in all three directions, all unequal lengths must be stated to completely define the crystal. The same is true if all axial angles are not equal.

Face-Centered Cubic System. The fcc system is shown in Fig. A.10. As the name implies, in addition to the corner atoms, there is an atom centrally located on each face. Because each of the atoms located on the faces belongs to two unit cells and the eight corner atoms each belong to eight unit cells, the number of atoms belonging to a unit cell is four. The atomic packing factor (the volume of atoms belonging to the unit cell divided by the volume of the unit cell) is 0.74 for the fcc structure. This is the densest packing that can be obtained. The fcc structure is the most efficient, with 12 nearest atom neighbors (also referred to as the coordination number, CN), that is, the fcc structure has a $\text{CN} = 12$. As shown in Fig. A.11, the stacking sequence for the fcc structure is *ABCABC*. The fcc structure is found in many important metals such as aluminum, copper, and nickel.

Hexagonal Close-Packed System. The atoms in the hcp structure (Fig. A.12) are also packed along close-packed planes. It should also be noted that both the fcc and hcp structures are what is known as close-packed

Table A.2 Seven crystal systems

Crystal system	Edge lengths	Interaxial angles
Triclinic	$a \neq b \neq c$	$\alpha \neq \beta \neq \gamma \neq 90^\circ$
Monoclinic	$a \neq b \neq c$	$\alpha = \gamma = 90^\circ \neq \beta$
Orthorhombic	$a \neq b \neq c$	$\alpha = \beta = \gamma = 90^\circ$
Tetragonal	$a = b \neq c$	$\alpha = \beta = \gamma = 90^\circ$
Hexagonal	$a = b \neq c$	$\alpha = \beta = 90^\circ, \gamma = 120^\circ$
Rhombohedral	$a = b = c$	$\alpha = \beta = \gamma \neq 90^\circ$
Cubic	$a = b = c$	$\alpha = \beta = \gamma = 90^\circ$

Source: Ref A.1

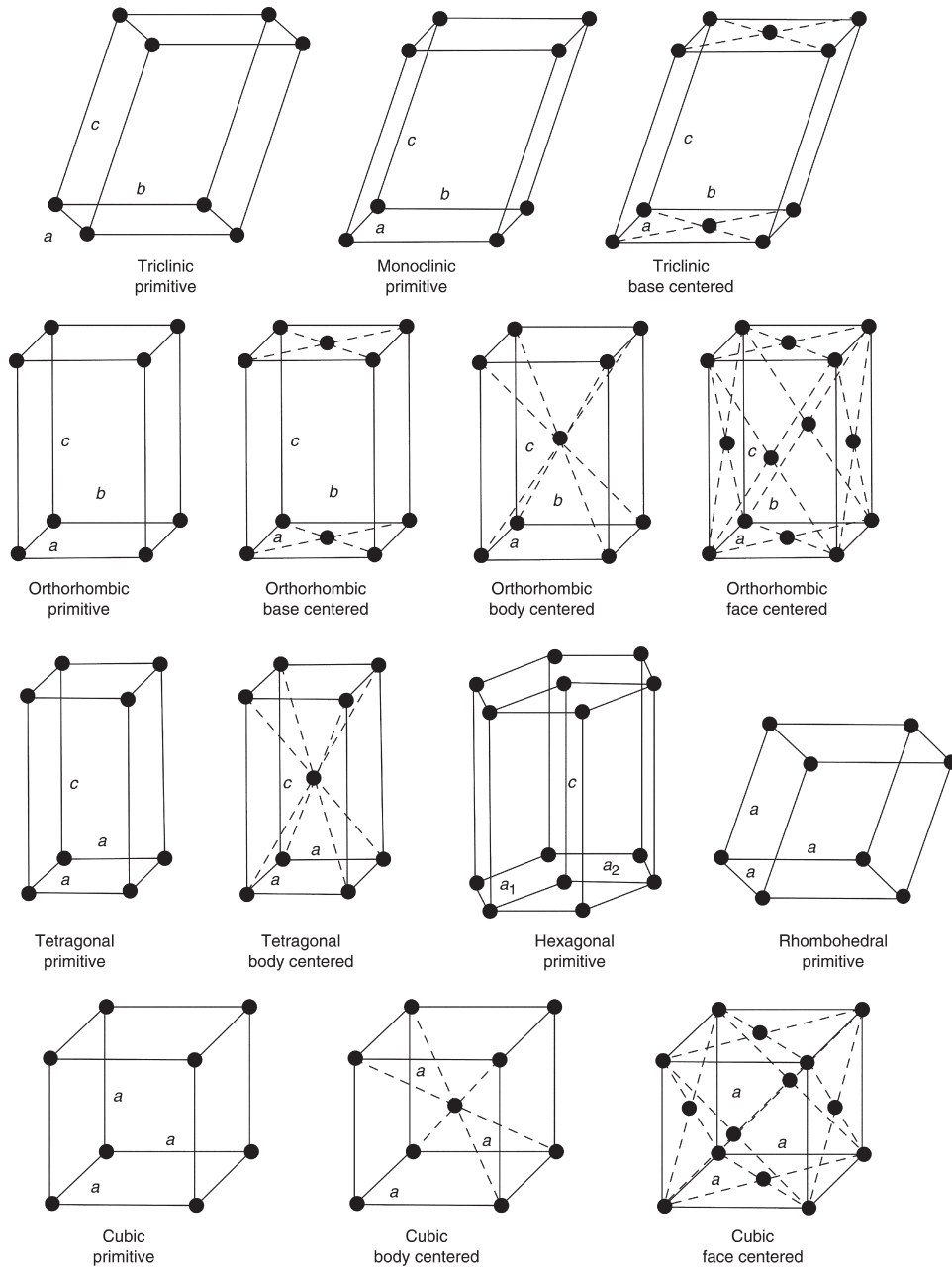


Fig. A.8 The fourteen Bravais lattices. Source: Ref A.1

structures with crystallographic planes having the same arrangement of atoms, however, the order of stacking the planes is different. Atoms in the hcp planes (called the basal planes) have the same arrangement as those in the fcc close-packed planes. However, in the hcp structure, these planes repeat every other layer to give a stacking sequence of ...*ABA*... . The

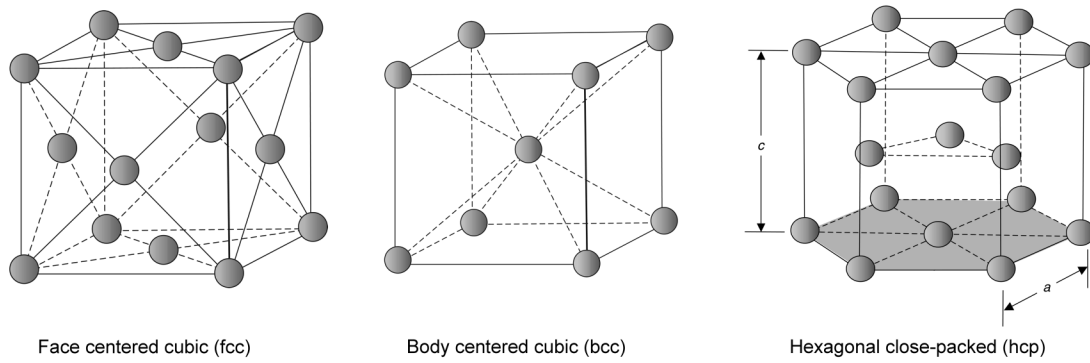


Fig. A.9 Common metallic crystalline structures. Source: Ref A.1

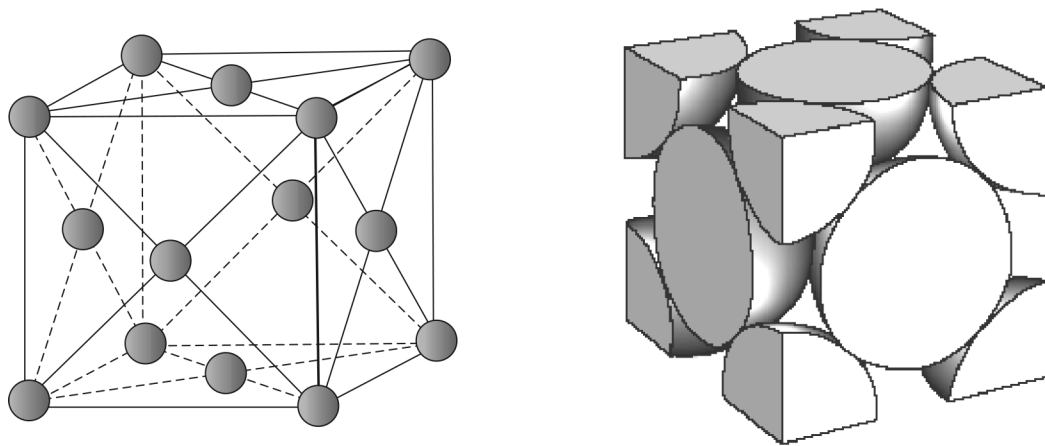


Fig. A.10 Face-centered cubic (fcc) structure. Source: Ref A.1

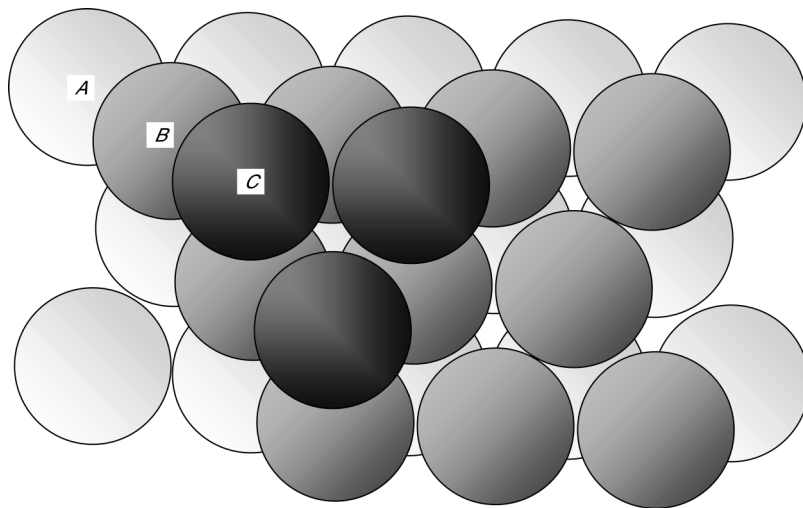


Fig. A.11 Close packing of planes. Source: Ref A.1

number of atoms belonging to the hcp unit cell is six and the atomic packing factor is 0.74. Note that this is the same packing factor as was obtained for the fcc structure. Also, the CN obtained for the hcp structure, 12, is the same as that for the fcc structure. A basic rule of crystallography is that if the CNs of two different unit cells are the same, then they will both have the same packing factors.

Two lattice parameters, c and a , also shown in Fig. A.12, are needed to completely describe the hcp unit cell. In an ideal hcp structure, the ratio of the lattice constants c/a is 1.633. In this ideal packing arrangement, the layer between the two basal planes in the center of the structure is located

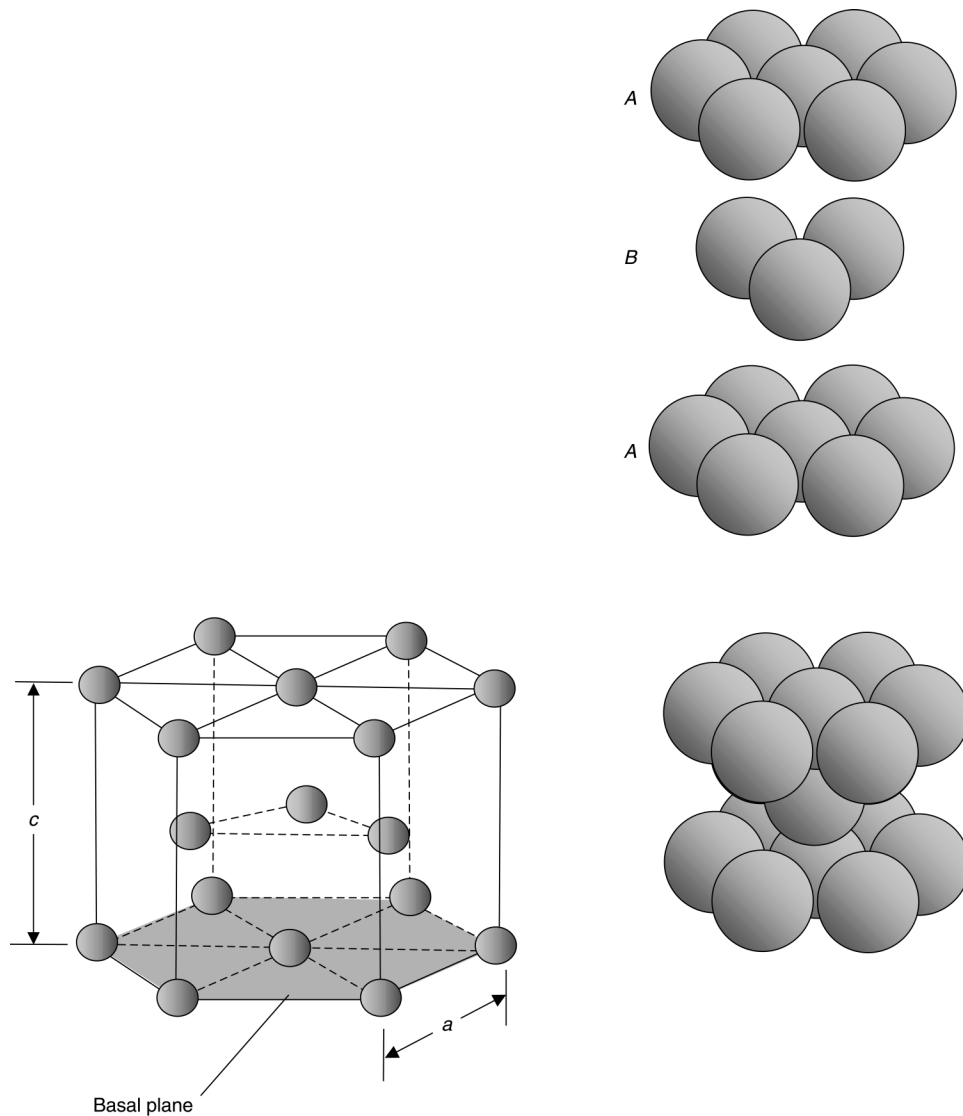


Fig. A.12 Hexagonal close-packed (hcp) structure. Source: Ref A.1

close to the atoms on the upper and lower basal planes. Therefore, any atom in the lattice is in contact with 12 neighboring atoms, and therefore $CN = 12$. It should be noted that there is often some deviation from the ideal ratio of $c/a = 1.633$. If the ratio is less than 1.633, it means that the atoms are compressed in the c -axis direction, and if the ratio is greater than 1.633, the atoms are elongated along the c -axis. In these situations, the hcp structure can no longer be viewed as truly being close packed and should be described as just being hexagonal. However, structures deviating from the ideal packing are still normally described as being hcp. For example, beryllium is described as having an hcp structure, but its c/a ratio of 1.57 is unusually low and causes some distortion in the lattice. This distortion and the unusually high elastic modulus of beryllium (3×10^5 MPa, or 42×10^3 ksi) result from a covalent component in its bonding. Contributions from covalent bonding are also present in the hcp metals zinc and cadmium, with c/a ratios greater than 1.85. This lowers their packing density to approximately 65%, considerably less than the 74% of the ideal hcp structure.

Body-Centered Cubic System. The body-centered cubic (bcc) system is shown in Fig. A.13. The bcc system is similar to the simple cubic system except that it has an additional atom located in the center of the structure. Because the center atom belongs completely to the unit cell in question, the number of atoms belonging to the bcc unit cell is two. The CN for the bcc structure is eight, because the full center atom is in contact with eight neighboring atoms located at the corner points of the lattice. The atomic packing factor for the bcc structure is 0.68, which is less than that of the fcc and hcp structures. Because the packing is less efficient in the bcc structure, the closest-packed planes are less densely packed (Fig. A.14).

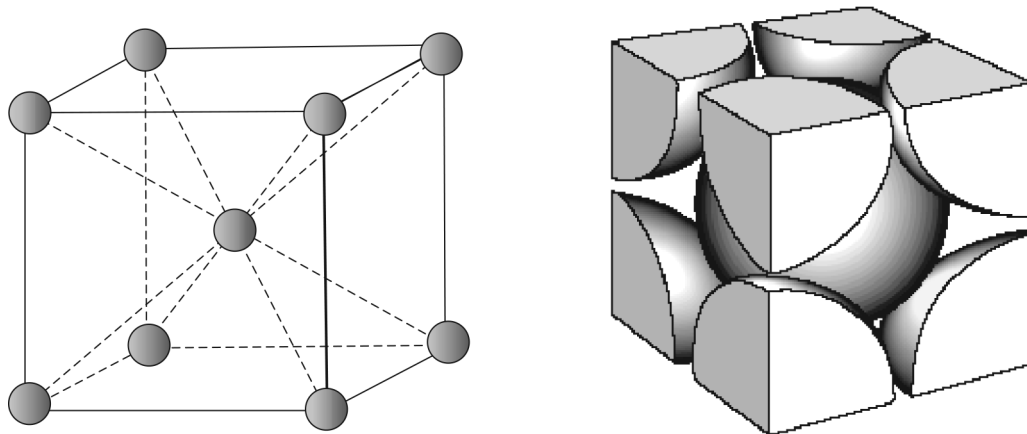


Fig. A.13 Body-centered cubic (bcc) structure. Source: Ref A.1

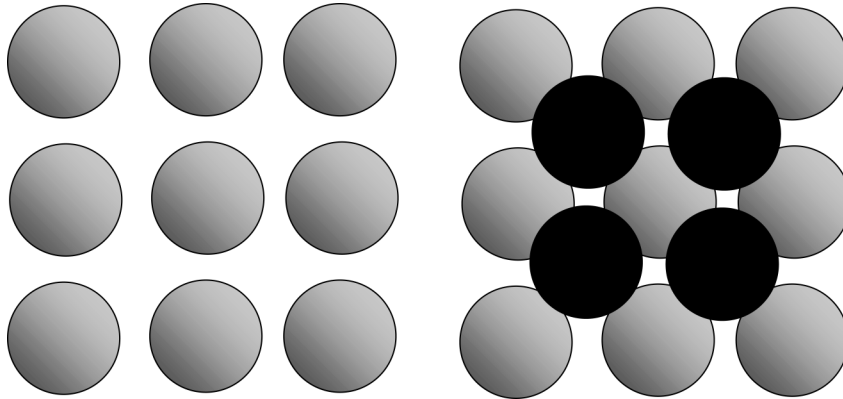


Fig. A.14 Loose packing in bcc structure. Source: Ref A.1

Even though the bcc crystal is not a densely packed structure, it is the equilibrium structure of 15 metallic elements at room temperature, including many of the important transition elements. This is attributable to two factors: (1) Even though each atom has only eight nearest neighbors, the six second-nearest neighbor atoms are closer in the bcc structure than in the fcc structure. Calculations indicate that these second-nearest neighbor bonds make a significant contribution to the total bonding energy of bcc metals; and (2) in addition, the greater entropy of the less densely packed bcc structure gives it a stability advantage over the more tightly packed fcc structure at high temperatures. As a consequence, some metals that have the close-packed structures at room temperature transition to bcc structures at higher temperatures.

A.4 Crystalline System Calculations

The atomic packing factor (APF) and coordination number (CN) of the important crystalline structures can be calculated from their geometries.

Cubic Systems. The cubic crystal systems are regular cubes with a lattice parameter such that $a = b = c$ and $\alpha = \beta = \gamma = 90^\circ$. Therefore, only one lattice parameter (a) is required to define the cubic lattice. Within the cubic family of systems, there are three important variations: (1) the simple or primitive cubic, in which there are atoms only at the corner points of the lattice, (2) the body-centered cubic (bcc) structure, which has an additional atom located at the center of the structure, and (3) the face-centered cubic (fcc) structure, which has an extra atom located on each of the six faces. The bcc and fcc structures are extremely important in metallurgy, with about 90% of industrially important metals crystallizing into one of these two structures.

Simple Cubic System. Two types of graphical depictions of a simple cubic system are shown in Fig. A.15, namely, the point model and the hard ball model. Although the hard ball model, with the outermost electron shells in contact, is the more realistic of the two, the point model is more commonly used because it is easier to visualize all of the atoms.

The relationship between the atomic radius, r , and the lattice constant, a , is shown in Fig. A.15 and is equal to:

$$a = 2r \quad (\text{Eq A.1})$$

Another important value is the number of atoms, N , belonging to a unit cell. Examination of the hard ball model of Fig. A.15 reveals that each atom located at the corner point of the unit cell belongs to eight unit cells. Therefore, only $1/8$ of each atom can be considered to belong to one unit cell. Because there are eight corners, or atomic positions, in the unit cell, the number of atoms belonging to the unit cell is:

$$N = 8 \left(\frac{1}{8} \right) = 1 \quad (\text{Eq A.2})$$

Thus, in a simple cubic crystal system, one full atom belongs to each unit cell.

In metals, the atoms tend to pack or occupy positions as close as possible to each other and to form the most dense lattice structure possible. The APF, which indicates the part of the volume of the unit cell that is actually occupied by atoms, is used to describe the denseness of the unit cell.

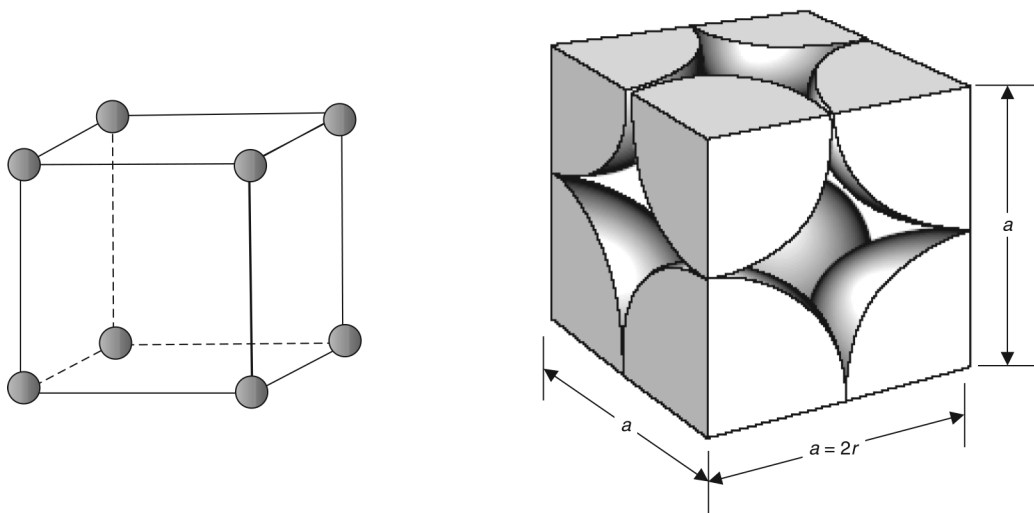


Fig. A.15 Simple cubic structure. Source: Ref A.1

$$\text{APF} = \frac{V_a}{V_c} = \frac{\text{Volume of atoms belonging to unit cell}}{\text{Volume of unit cell}} \quad (\text{Eq A.3})$$

The volume of atoms belonging to the simple unit cell can be calculated as:

$$V_a = N \frac{4\pi r^3}{3} \quad (\text{Eq A.4})$$

Likewise, the volume of the simple cubic system is:

$$V_c = a^3 = 8r^3 \quad (\text{Eq A.5})$$

Therefore, the APF is:

$$\text{APF} = \frac{N \frac{4\pi r^3}{3}}{8r^3} = \frac{N\pi}{6} \quad (\text{Eq A.6})$$

Because $N = 1$ for the simple cubic system, the APF reduces to:

$$\text{APF} = \frac{\pi}{6} = 0.52 \quad (\text{Eq A.7})$$

This means that only approximately half of the simple cubic system is occupied with atoms. Because metals tend to pack as closely as possible during crystallization, this rather loose packing explains why very few metals crystallize into the simple cubic system.

Another parameter used to define crystal systems is the CN, or number of nearest neighboring atoms each atom in the structure possesses. In the hard ball model, it is the number of atoms that touch a given atom. Referring again to Fig. A.15, it can be seen that any atom is in contact with six neighboring atoms, thus $\text{CN} = 6$.

Body-Centered Cubic System. The body-centered cubic (bcc) system is shown in Fig. A.16. The bcc system is similar to the simple cubic system except that it has an additional atom located in the center of the structure. Because the center atom belongs completely to the unit cell in question, the number of atoms belonging to the bcc unit cell is:

$$N = 8 \times \frac{1}{8} + 1 = 2 \quad (\text{Eq A.8})$$

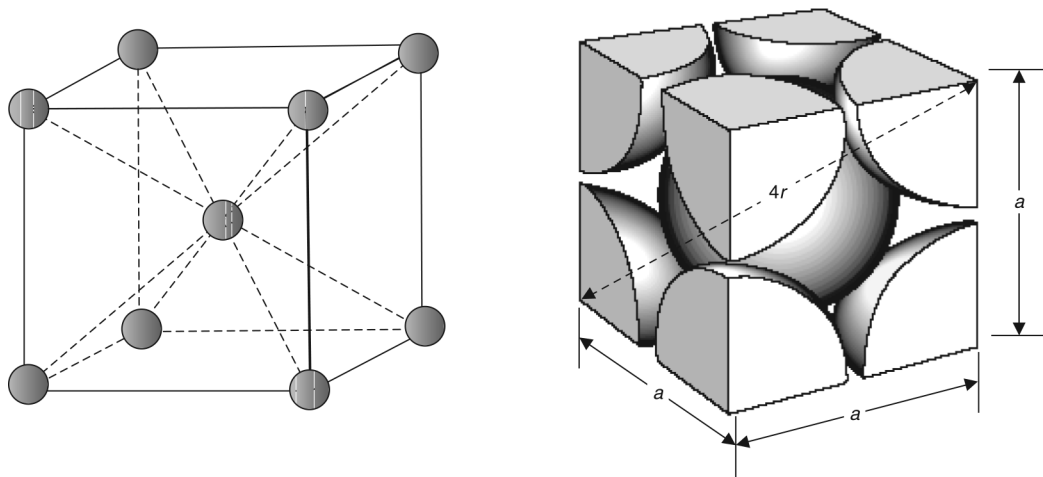


Fig. A.16 Body-centered cubic structure. Source: Ref A.1

The relationship between the lattice parameter, a , and the atomic radius, r , is:

$$a = \frac{4r}{\sqrt{3}} \quad (\text{Eq A.9})$$

The APF can then be calculated to be:

$$\text{APF} = \frac{\frac{4N\pi r^3}{3}}{a^3} = \frac{\frac{4N\pi r^3}{3}}{\frac{64r^3}{3\sqrt{3}}} \quad (\text{Eq A.10})$$

$$\text{APF} = \frac{\pi\sqrt{3}}{8} = 0.68 \quad (\text{Eq A.11})$$

Because the APF for the bcc structure is significantly higher (0.68) than that for the simple cubic structure (0.52), the bcc structure is significantly denser and many important metals, α -iron for example, crystallize into the bcc structure.

For the bcc structure, CN = 8, because the full center atom is in contact with eight neighboring atoms located at the corner points of the lattice.

Face-Centered Cubic System. The face-centered cubic (fcc) system is shown in Fig. A.17. As the name implies, in addition to the corner atoms,

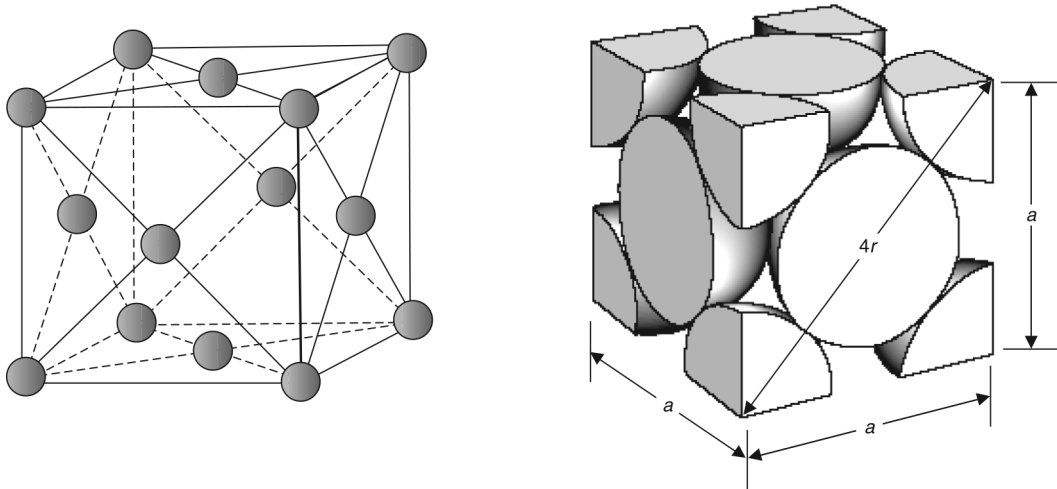


Fig. A.17 Face-centered cubic structure. Source: Ref A.1

there is an atom centrally located on each face. Because each of the atoms located on the faces belong to two unit cells and the eight corner atoms each belong to eight unit cells, the number of atoms belonging to a unit cell is:

$$N = 8 \times \frac{1}{8} + 6 \times \frac{1}{2} = 4 \quad (\text{Eq A.12})$$

Because, in the fcc structure, atoms are in contact along the face diagonals, the relationship between the lattice parameter and atomic radius is:

$$a = \frac{4r}{\sqrt{2}} \quad (\text{Eq A.13})$$

The APF can then be calculated as:

$$\text{APF} = \frac{\frac{4N\pi r^3}{3}}{a^3} = \frac{\frac{4N\pi r^3}{3}}{\frac{64r^3}{2\sqrt{2}}} \quad (\text{Eq A.14})$$

Substituting $N = 4$ into the equation, the APF becomes:

$$\text{APF} = \frac{\pi\sqrt{2}}{6} = 0.74 \quad (\text{Eq A.15})$$

Because 74% of the fcc lattice is occupied by atoms, this is an even denser packing than that for the bcc structure. It occurs in many important metals such as aluminum, copper, and nickel.

The fcc structure has a CN = 12. With 12 nearest atom neighbors, the fcc structure is the most efficient of the cubic structures.

Hexagonal System. The hexagonal close-packed (hcp) system is shown in Fig. A.18. The lattice parameters are:

$$a_1 = a_2 = a_3 \neq c$$

$$\alpha_1 = \alpha_2 = \alpha_3 = 120^\circ; \gamma = 90^\circ$$

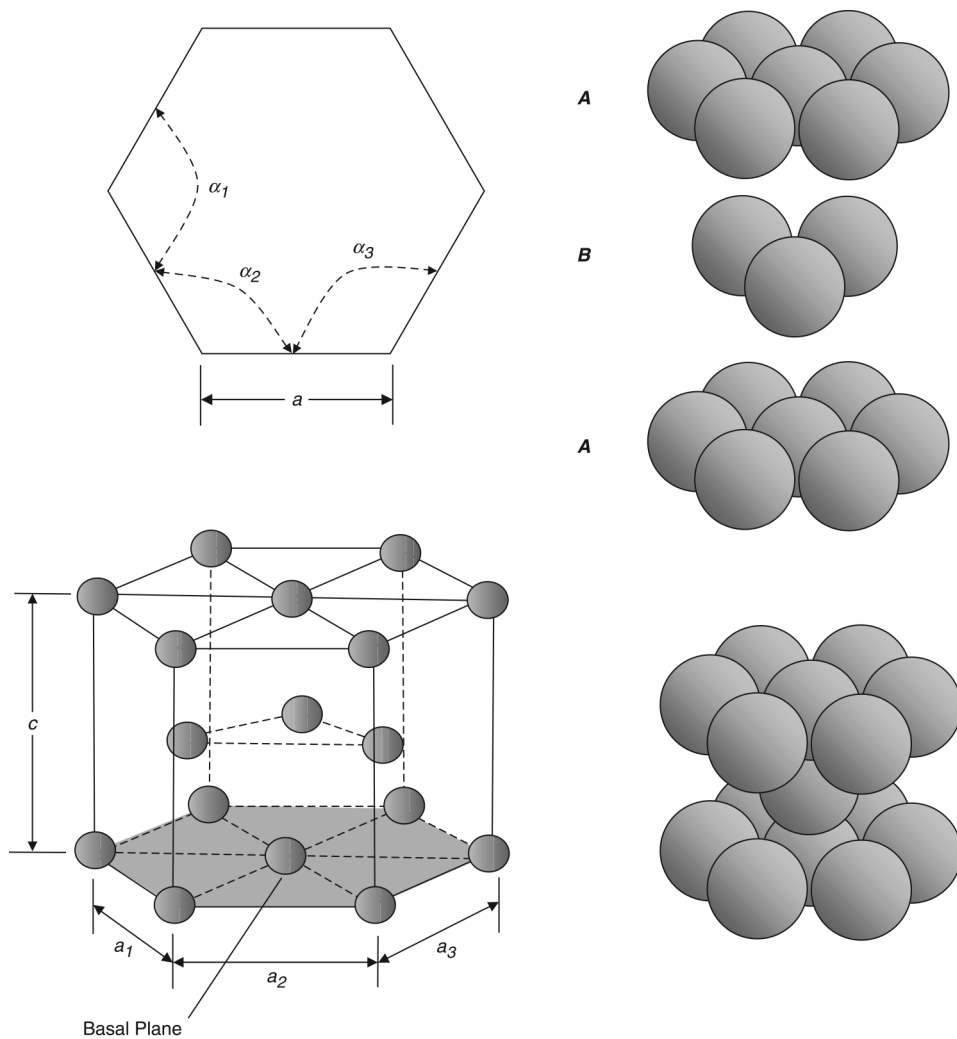


Fig. A.18 Hexagonal closed-packed structure. Source: Ref A.1

To determine the number of atoms belonging to a unit cell, note that atoms at the corner points belong to the six neighboring lattices and they contribute $1/6$ of an atom to the unit cell. Atoms at the face centers belong to two adjacent lattices and contribute $1/2$ of an atom to the unit cell. Finally, the three atoms in the interior all belong to the unit cell. The number of atoms belonging to the unit cell is therefore:

$$N = 12 \times \frac{1}{6} + 2 \times \frac{1}{2} + 3 \times 1 = 6 \quad (\text{Eq A.16})$$

In an ideal hcp structure, the ratio of the lattice constants c/a is 1.633. In this ideal packing arrangement, the layer between the two basal planes in the center of the structure is located close to the atoms on the upper and lower basal planes. Therefore, any atom in the lattice is in contact with 12 neighboring atoms and therefore $CN = 12$. It should be noted that there is often some deviation from the ideal ratio of $c/a = 1.633$. If the ratio is less than 1.633, it means that the atoms are compressed in the c -axis direction, and if the ratio is greater than 1.633, the atoms are elongated along the c -axis.

The relationships between the lattice parameters, a and c , and the atomic radius, r , for an ideal hcp structure ($c/a = 1.633$) are:

$$\begin{aligned} a &= 2r \\ c &= 1.6333 \times 2r = 3.266r \end{aligned} \quad (\text{Eq A.17})$$

To determine the atomic packing factor, first determine the volume of the hexagonal lattice using Fig. A.19. The area of the base hexagon is:

$$A = 3a^2 \sin 60^\circ = \frac{3\sqrt{3}}{2} a^2 \quad (\text{Eq A.18})$$

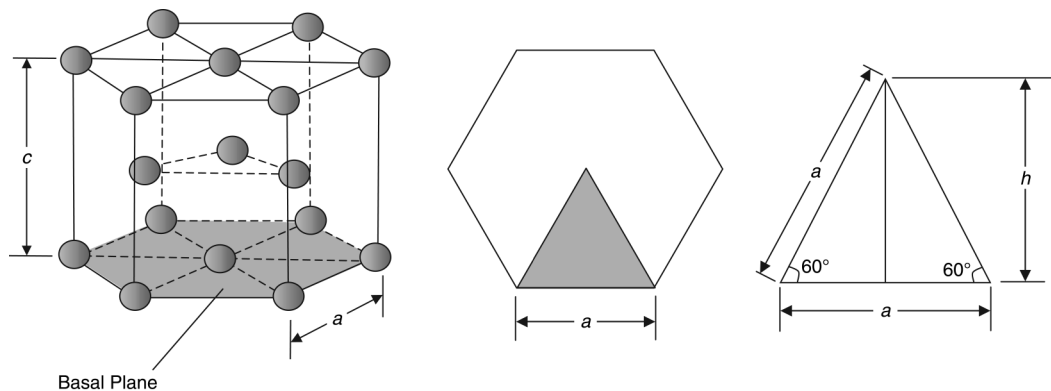


Fig. A.19 Calculation of volume of hexagonal lattice. Source: Ref A.1

The volume of the lattice is:

$$V_c = \frac{3\sqrt{3}}{2} 1.633a^3 \quad (\text{Eq A.19})$$

The APF is then:

$$\text{APF} = \frac{V_a}{V_c} = \frac{4N\pi r^3}{\frac{3\sqrt{3}}{2} 1.633a^3} \quad (\text{Eq A.20})$$

Substituting $a = 2r$ in Eq A.20 gives:

$$\text{APF} = \frac{N\pi}{(1.633)9\sqrt{3}} \quad (\text{Eq A.21})$$

Finally, substituting the number of atoms belonging to the unit cell, $N = 6$, gives:

$$\text{APF} = 0.74 \quad (\text{Eq A.22})$$

Note that this is the same value as was obtained for the fcc structure. Also, the CN obtained for the fcc structure, 12, is the same as that for the hcp structure. A basic rule of crystallography is that if the CNs of two different unit cells are the same, then they will both have the same packing factors. It should also be noted that both the fcc and hcp structures are what is known as close-packed structures with crystallographic planes having the same arrangement of atoms; however, the order of stacking the planes is different.

A.5 Slip Systems

Plastic deformation takes place by sliding (slip) of close-packed planes over one another. A reason for this slip plane preference is that the separation between close-packed planes is greater than for other crystal planes, and this makes their relative displacement easier. Furthermore, the slip direction is in a close-packed direction. The combination of planes and directions on which slip takes place constitutes the slip systems of the material. In polycrystalline materials, a certain number of slip systems must be available in order for the material to be capable of plastic deformation. Other things being equal, the greater the number of slip systems, the greater the capacity for deformation. Face-centered cubic metals have

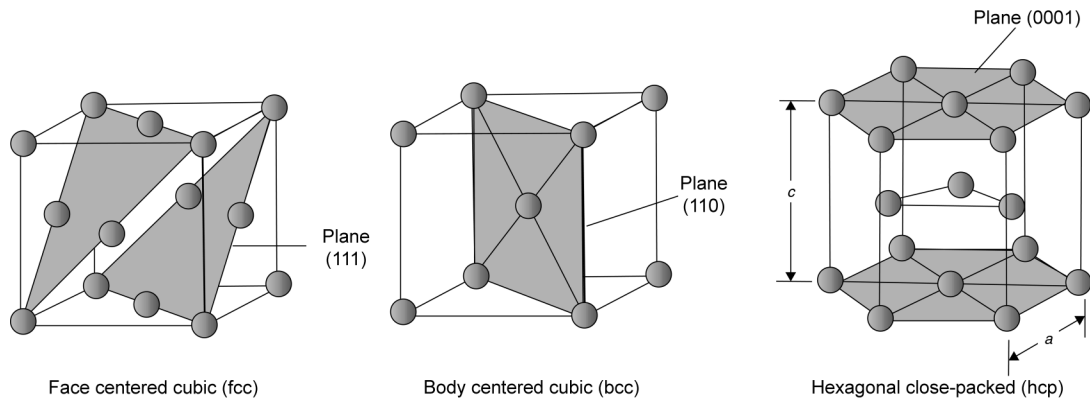


Fig. A.20 Close-packed planes. Source: Ref A.1

a large number of slip systems (12) and are capable of moderate to extensive plastic deformation even at temperatures approaching absolute zero. A number of close-packed planes for the fcc, bcc, and hcp structures are illustrated in Fig. A.20.

Materials having the bcc structure also often display 12 slip systems, although this number comes about differently than it does for the fcc lattice. A closest-packed bcc plane is defined by a unit cell edge and face diagonal. There are only two close-packed directions (the cube diagonals) in the closest-packed bcc plane, but there are six nonparallel planes of this type. Over certain temperature ranges, some bcc metals display slip on other than close-packed planes, although the slip direction remains a close-packed one. Thus, bcc metals have the requisite number of slip systems to allow for plastic deformation. However, bcc metals often become brittle at low temperatures as a result of the strong temperature sensitivity of their yield strength, which causes them to fracture prior to undergoing significant plastic deformation.

Depending on their c/a ratio, polycrystalline hcp metals may or may not have the necessary number of slip systems to allow for appreciable plastic deformation. The ideal hcp structure has only three slip systems, because there is only one nonparallel close-packed plane in it (the basal plane, which contains three nonparallel close-packed directions). However, three slip systems are insufficient to permit polycrystalline plastic deformation, and so hcp polycrystals for which slip is restricted to the basal plane are not malleable. When c/a is less than the ideal ratio, basal planes become less widely separated, and other planes compete with them for slip activity. In these instances, the number of slip systems increases, and material ductility is beneficially affected. In addition, polycrystalline hcp metals can also deform by a mechanism called twinning.

A.6 Crystallographic Planes and Directions

This section will give a short introduction to identifying crystalline planes and crystalline directions.

Miller Indices for Cubic Systems. Special planes and directions within metal crystal structures play an important part in plastic deformation, hardening reactions, and other aspects of metal behavior. Crystallographic planes are defined by what are called Miller indices. Consider the general plane shown in Fig. A.21. The Miller indices for a given plane can be determined as follows:

1. The plane should be displaced, if necessary, with a parallel displacement to a position where it does not pass through the origin of the coordinate system. This is permissible because (1) the coordinate system chosen is an arbitrary one that could be chosen anywhere on the vast expanse of a space lattice, and (2) as we shall see, parallel planes are equivalent.
2. The a , b , and c intercepts of the plane with the x , y , and z coordinates are determined.
3. The reciprocals of these numbers are determined. The reciprocals are denoted by the letters h , k , l , respectively:

$$\frac{1}{a} \rightarrow h; \frac{1}{b} \rightarrow k; \frac{1}{c} \rightarrow l$$

4. The reciprocals normally result in fractions. Apply either multiplication or division to determine the smallest set of h , k , and l values that yield integer numbers. These numbers, when enclosed in brackets such as $(h\ k\ l)$, give the Miller indices for the plane.

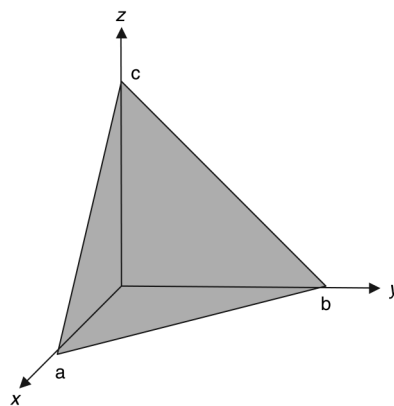


Fig. A.21 Crystallographic plane indices for cubic systems. Source: Ref A.1

Several examples can be used to best show the calculation method. The Miller indices for the plane shown in Fig. A.22(a) would be:

1. Intercepts $x = 1, y = 1, z = 1$
2. Reciprocals $\frac{1}{x} = 1, \frac{1}{y} = 1, \frac{1}{z} = 1$
3. No fractions to clear
4. (111)

The Miller indices for the plane shown in Fig. A.22(b) would be:

1. The plane never intercepts the z -axis, so $x = 1, y = 2, z = \infty$.
2. Reciprocals $\frac{1}{x} = 1, \frac{1}{y} = \frac{1}{2}, \frac{1}{z} = \frac{1}{\infty} = 0$
3. Clear fractions $\frac{1}{x} = 2, \frac{1}{y} = 1, \frac{1}{z} = \frac{1}{\infty} = 0$
4. (210)

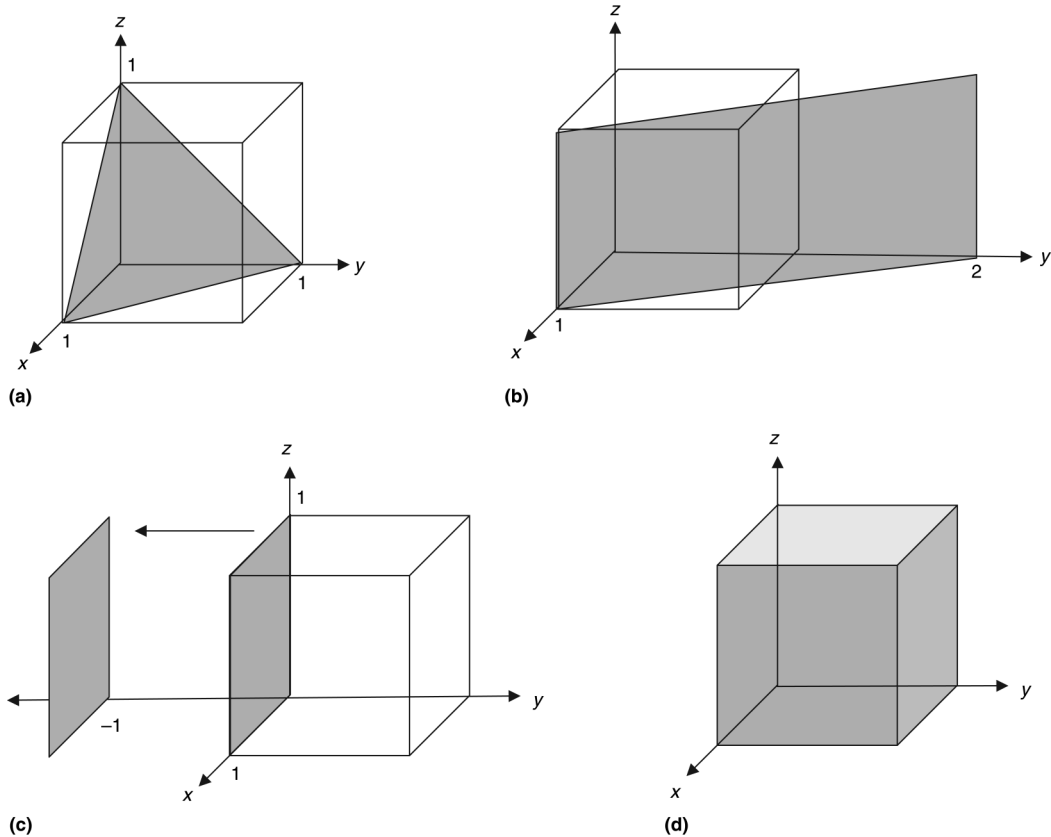


Fig. A.22 Examples of Miller indices for planes. Source: Ref A.1

The Miller indices for the plane shown in Fig. A.22(c) would be:

1. Because the plane passes through the origin, the plane must be moved. If it is moved one lattice parameter in the y -direction, the $x = \infty$, $y = -1$, $z = \infty$.
2. Reciprocals $\frac{1}{x} = 0$, $\frac{1}{y} = -1$, $\frac{1}{z} = 0$
3. No fractions to clear
4. $(0\bar{1}0)$ Note that the negative intercept of -1 for the y -axis has a bar placed over the top of it (i.e., $\bar{1}$).

Finally, examine Fig. A.22(d) in which all of the side faces of the cube are indicated with planes. Remembering that the space lattice, for all purposes, is infinite in all three coordinate directions, and that our designation of the coordinate system, x , y , and z , is also arbitrary, it can be concluded that all of the face planes in the cube shown have the same atomic arrangement. These are known as crystallographic equivalent planes. A little analysis will show that all of these planes consist of the same three numbers, namely $1,0,0$. Crystallographic equivalent planes are known as family planes and are denoted by putting the integers in braces. In this case, the notation $\{100\}$ represents all side faces of the cube collectively as a family plane.

Miller-Bravais Indices for Hexagonal Crystal Systems. The hexagonal crystal systems use a slightly different procedure for specifying the crystalline planes. Besides the h , k , and l indices, there is a fourth index, i , that is used for hexagonal systems. In the Miller-Bravais system, the three axes in the basal plane are denoted by a_1 , a_2 , and a_3 indices, while l is used to denote the intercept with the z -axis. Thus, a plane will have the designation $(h\ k\ i\ l)$. As mentioned earlier, there are two different lattice parameters. The lattice parameter a is measured along the three axes of the basal plane, while the c -axis is measured in the direction of the z -axis perpendicular to the basal plane. Thus, $a_1 = a_2 = a_3 = a \neq c$.

The Miller indices for the basal plane shown in Fig. A.23(a) would be:

1. Intercepts $a_1 = a_2 = a_3 = \infty$; $c = 1$
2. Reciprocals $\frac{1}{a_1} = \frac{1}{a_2} = \frac{1}{a_3} = 0$; $\frac{1}{c} = 1$
3. No fractions to clear
4. (0001)

The Miller indices for the basal plane shown in Fig. A.23(b) would be:

1. Intercepts $a_1 = 1$, $a_2 = 1$, $a_3 = -\frac{1}{2}$; $c = 1$

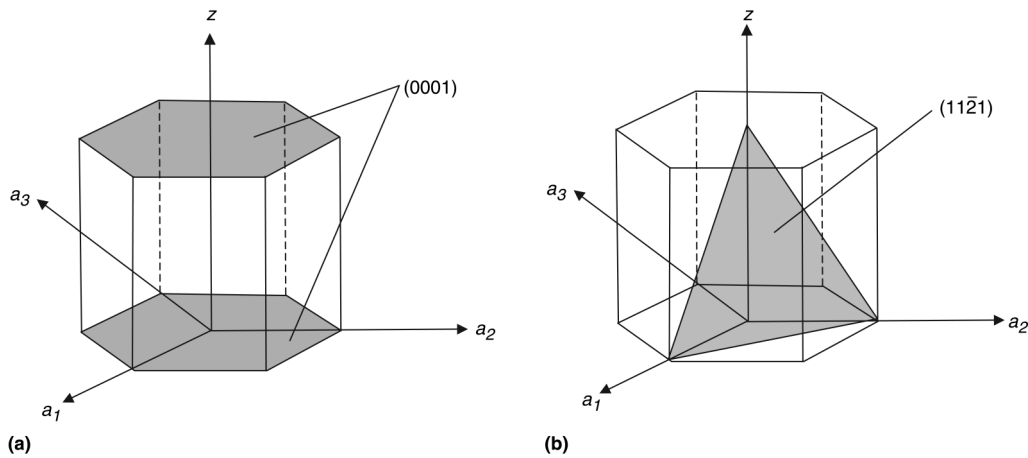


Fig. A.23 Examples of Miller-Bravais indices for hexagonal planes. Source: Ref A.1

2. Reciprocals $\frac{1}{a_1} = 1, \frac{1}{a_2} = 1, \frac{1}{a_3} = -2; \frac{1}{c} = 1$
3. No fractions to clear
4. $(11\bar{2}1)$

Because the four axes representation contains redundancy, the equation $h + k = -i$ is valid for the indices. In other words, the third index in the basal plane can be calculated from the other two.

Crystallographic Directions in Cubic Crystal Structures. A direction in a crystal is indicated by bracketed indices, for example, $[110]$, and in the cubic system, the direction is always perpendicular to the plane having the same indices (Fig. A.24). More generally, a line in a given direction, such as $[110]$, can be constructed in the following manner. Draw a line from the origin through the point having the coordinates $x = 1, y = 1, z = 0$, in terms of axial lengths. This line and all lines parallel to it are then in the given direction. Note that reciprocals are not involved in obtaining the Miller indices of directions. A family of equivalent directions, such as $[100], [\bar{1}00], [010], [0\bar{1}0], [001],$ and $[00\bar{1}]$, is designated as $\{100\}$.

Crystallographic Directions in Hexagonal Crystal Structures. The direction system for the Miller-Bravais system for hexagonal crystal structures is extremely cumbersome and confusing. An explanation is attempted here, and then its use will be avoided whenever possible. Miller-Bravais indices of direction are also expressed in terms of four digits. Like the indices for planes, the third digit must always equal the negative sum of

the first two digits (i.e., $h + k = -i$). Thus, if the first two digits are 2 and -1, then the third digit must be -1; that is, $(2) + (-1) = 1 \rightarrow -1$. The method for finding the direction of the a_1 axis is shown in Fig. A.25. This axis has the same direction as the vector sum of the three vectors, one of them of

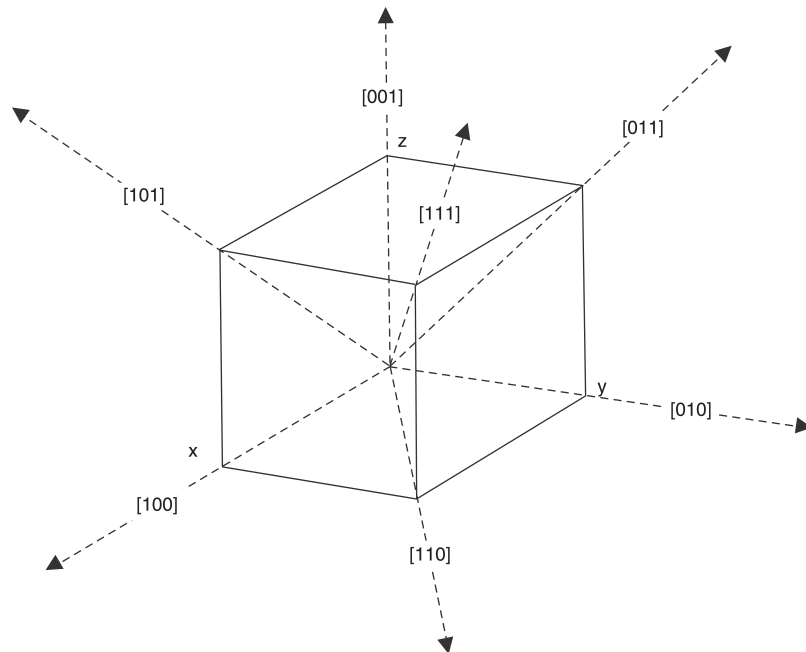


Fig. A.24 Important directions in a cubic cell. Source: Ref A.1

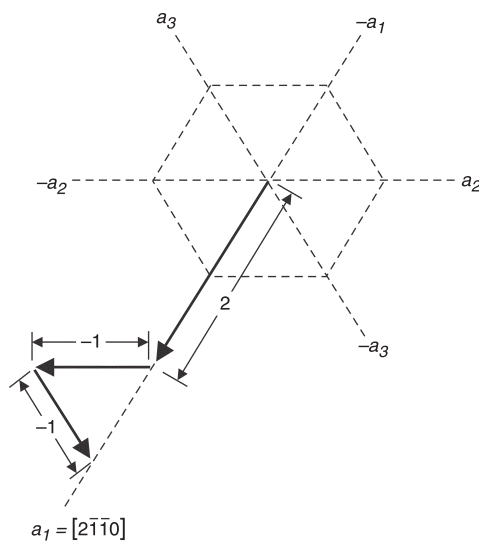


Fig. A.25 Example of Miller-Bravais directional indices for hexagonal planes. Source: Ref A.3 as published in Ref A.1

length +2 along the a_1 axis, another of length -1 along the a_2 axis, and the third of length -1 along the a_3 axis. This yields direction indices of $[2\bar{1}\bar{1}0]$. This cumbersome method is required to satisfy the relationship $h + k = -i$. The corresponding indices of the a_2 and a_3 axes are $[\bar{1}2\bar{1}0]$ and $[\bar{1}\bar{1}20]$, respectively.

A.7 X-ray Diffraction for Determining Crystalline Structure

X-rays are a form of electromagnetic radiation that has high energies and short wavelengths. Because the wavelengths of x-rays are approximately the same as the atomic spacings on metallic lattices, a number of x-ray techniques have been developed over the years to determine crystalline structure. Diffraction occurs when a wave encounters a series of regularly spaced obstacles that (1) are capable of scattering the wave, and (2) have spacings that are comparable in magnitude to the wavelength. A diffracted beam is one in which a large number of scattered waves mutually reinforce one another.

When a beam of x-rays with a wavelength λ strikes at set of crystalline planes at some arbitrary angle, there will usually be no reflected beam because the rays reflected from the various crystal planes must travel paths of different lengths. In other words, although the incident rays are in phase, the reflected rays are out of phase and thus cancel one another. However, if each ray is out of phase with the preceding one by exactly one wavelength, or any whole integer wavelength ($n = 1, 2, 3, \dots$), then the reflected beam will consist of rays that are in phase again. The angle at which reflection occurs is known as the Bragg angle, θ .

Two parallel planes of atoms identified as $A-A'$ and $B-B'$, which have the same h, k, l Miller indices separated by the interplanar spacing d_{hkl} , are shown in Fig. A.26. Two in-phase rays, labeled 1 and 2, having a wavelength λ strike the surface at an angle θ . On impact, rays 1 and 2 are scattered by atoms P and Q . Constructive interference of the scattered rays $1'$ and $2'$ occurs at an angle to the planes, if the path length difference between $1-P-1'$ and $2-Q-2'$ (i.e., $\overline{SQ} + \overline{QT}$) is equal to a whole number, n , of wavelengths. This condition for diffraction is:

$$\begin{aligned} n\lambda &= \overline{SQ} + \overline{QT} \\ n\lambda &= d_{hkl} \sin \theta + d_{hkl} \sin \theta \\ n\lambda &= 2d_{hkl} \sin \theta \end{aligned} \quad (\text{Eq A.23})$$

Equation A.23 is known as Bragg's law; also, n is the order of reflection, which may be any integer (1, 2, 3, ...) consistent with $\sin \theta$ not exceeding unity. Bragg's law is a simple expression relating the x-ray wavelength and interatomic spacing to the angle of the diffracted beam. If Bragg's law is

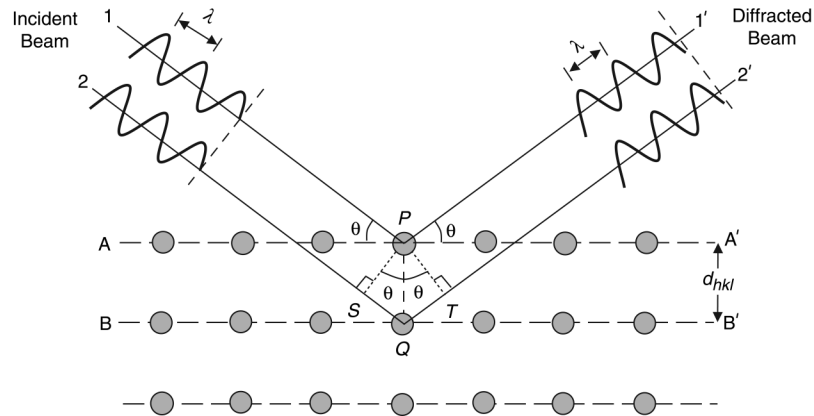


Fig. A.26 Diffraction of x-rays by planes of atoms. Source: Ref A.4 as published in Ref A.1

not satisfied, then the reflected rays will be out of phase and cancel each other. Although for a given metallic substance, n and d_{hkl} will ordinarily have only a few different values that will satisfy Bragg's law, the values for λ and θ can be varied continuously over a wide range.

The magnitude of the distance between two adjacent and parallel planes of atoms (i.e., the interplanar spacing d_{hkl}) is a function of the Miller indices (h , k , and l) as well as the lattice parameter(s). For example, for crystal structures that have cubic symmetry:

$$d_{hkl} = \frac{a}{\sqrt{h^2 + k^2 + l^2}} \quad (\text{Eq A.24})$$

in which a is the lattice parameter. There are also relationships similar to this one for the cubic system for the other crystalline systems.

There are a number of x-ray techniques that have been developed for studying crystalline structures. The Laue method uses a narrow collimated beam of white x-rays that strike a stationary single crystal. It is not suitable for the determination of lattice parameters but is used for the determination of crystal orientation and the detection of lattice imperfections. The rotating single-crystal method uses a constant wavelength beam while the diffracting crystal is rotated. This method is used mostly for determining the structure of single crystals. The Debye-Scherrer powder method uses an x-ray beam of constant wavelength and a specimen consisting of thousands of tiny crystals. Because there are a large number of powder particles with many different orientations, the diffracted beam produces a cone of radiation. Different reflection cones are recorded on a film strip that allows the diffraction angles to be measured. The distance d_{hkl} between the reflecting atomic planes is then calculated using Bragg's law.

In addition to the photographic methods, there are diffractometer methods that measure the intensity of the beam in counts per second diffracted from the specimen over a range of angles. A powdered or polycrystalline specimen consisting of many fine and randomly oriented particles is exposed to monochromatic x-radiation. Each powder particle (or grain) is a crystal, and having a large number of them with random orientations ensures that some particles are properly oriented such that every possible set of crystallographic planes will be available for diffraction. In a typical diffractometer (Fig. A.27), a specimen "S" is supported so that it rotates about the axis labeled "O." The monochromatic x-ray beam is generated at point "X," and the intensities of diffracted beams are detected with a counter labeled "C." The counter is mounted on a movable carriage that may also be rotated about the O-axis, with its angular position in terms of 2θ marked on a graduated scale. The carriage and specimen are mechanically coupled such that a rotation of the specimen through θ is accompanied by a 2θ rotation of the counter, which assures that the incident and reflection angles are maintained equal to one another. Collimators are incorporated within the beam path to produce a well-defined and focused beam. A filter provides a near-monochromatic beam. As the counter moves at constant angular velocity, a recorder automatically plots the diffracted beam intensity monitored by the counter as a function of 2θ , where 2θ is the diffraction angle and measured experimentally. A diffraction pattern for a powdered specimen of lead is shown in Fig. A.28. The high-intensity peaks result when the Bragg diffraction condition is satisfied by some set of crystallographic planes. One of the primary uses of x-ray diffractometry is for the determination of crystal structure. The unit cell size and geometry may be resolved from the angular positions of the diffraction peaks, while the arrangement of atoms within the unit cell is associated with the relative intensities of these peaks.

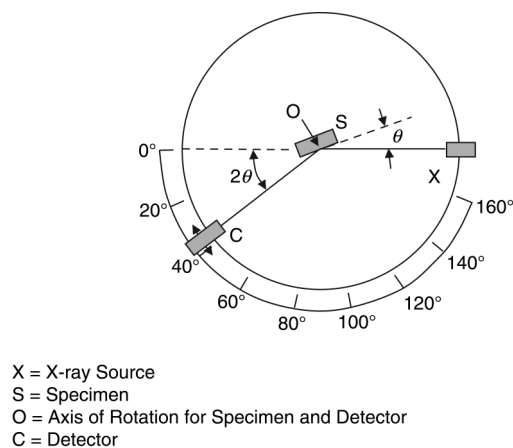


Fig. A.27 Schematic of x-ray diffractometer. Source: Ref A.4 as published in Ref A.1

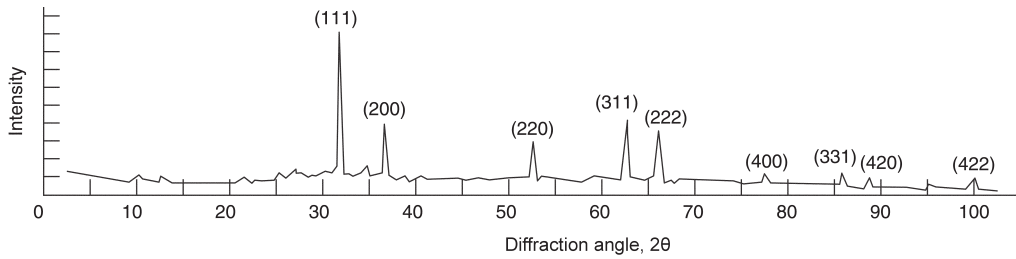


Fig. A.28 Typical diffraction pattern. Source: Ref A.4 as published in Ref A.1

A.8 Crystalline Imperfections

In a perfect crystalline structure, there is an orderly repetition of the lattice in every direction in space. However, real crystals are not perfect—they always contain a considerable number of imperfections, or defects, that affect their physical, chemical, mechanical, and electronic properties. It should be noted that defects do not necessarily have adverse effects on the properties of materials. They play an important role in processes such as deformation, annealing, precipitation, diffusion, and sintering.

All defects and imperfections can be conveniently classified under four main divisions: point defects, line defects, planar defects, and volume defects. Point defects are inherent to the equilibrium state and thus determined by temperature, pressure, and composition. However, the presence and concentration of the other defects depends on the way the metal was originally formed and subsequently processed.

Point Defects. A point defect is an irregularity in the lattice associated with a missing atom (vacancy), an extra atom (interstitial), or an impurity atom (substitutional). Due to their small size, point defects generally produce only very local distortions in the crystalline lattice. However, their presence can be significant, for example, in aiding diffusion in the crystalline lattice. Vacancies are the simplest defect. A vacancy is simply an atom missing from the crystalline lattice, as illustrated in Fig. A.29. Vacancies are created during solidification due to imperfect packing. They also occur during processing at elevated temperatures. In an otherwise completely regular lattice, the atoms are constantly being displaced from their ideal locations by thermal vibrations. The frequency of vibration is almost independent of temperature, but the amplitude increases with increasing temperature. For copper, the amplitude near room temperature is approximately one-half its value near the melting point and approximately twice its value near absolute zero. As the temperature is increased, the lattice vibrations become larger and atoms have a tendency to jump out of their normal positions, leaving a vacant lattice site behind.

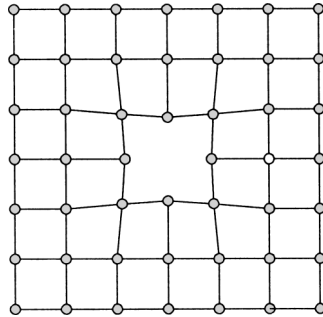


Fig. A.29 Vacancy point defect. Source: Ref A.5 as published in Ref A.1

The number of vacancies increases exponentially with temperature according to:

$$n_v = Ne^{-E_v/kT} \quad (\text{Eq A.25})$$

where n_v is the number of vacancies at temperature T , N is the total number of lattice sites, E_v is energy necessary to form a vacancy, K is Boltzmann's constant (1.38×10^{-24} J/K), and T is absolute temperature in degrees Kelvin.

While the number of vacancies would be zero at absolute zero, it is on the order of 10^{-3} for metals near their melting point. According to Eq A.25, at any temperature above absolute zero, the equilibrium condition for a metal will contain vacancies; that is, the presence of vacancies is a condition of equilibrium.

Vacancies affect the properties of the metal. Density slightly decreases as the number of vacancies increases. The electrical resistance also decreases as the number of vacancies increases. Vacancies enhance atomic diffusion. Vacancy diffusion is the movement of a vacancy through the lattice, thereby assisting the diffusion of atoms. The number of dislocations is reduced when the vacancies diffuse to grain boundaries or surfaces, which act as sinks. If a metal is heated to a high temperature, the number of vacancies increases. If it is then suddenly quenched to room temperature, the vacancies are trapped in the lattice because they do not have time to diffuse out.

Vacancies can form by several mechanisms. In the Frenkel mechanism (Fig. A.30), an atom is displaced from its normal lattice position into an interstitial site. However, this requires quite a bit of energy—the energy to form a vacancy and the energy to form an interstitial. Therefore, the probability is quite low. A more realistic, and lower-energy method, is the Schottky mechanism (Fig. A.31), in which vacancies originate at free surfaces and move by diffusion into the crystal interior.

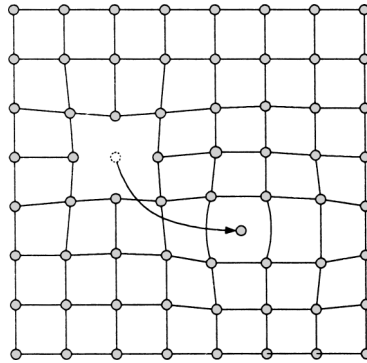


Fig. A.30 Frenkel mechanism. Simultaneous formation of vacancy and interstitial atom. Source: Ref A.5 as published in Ref A.1

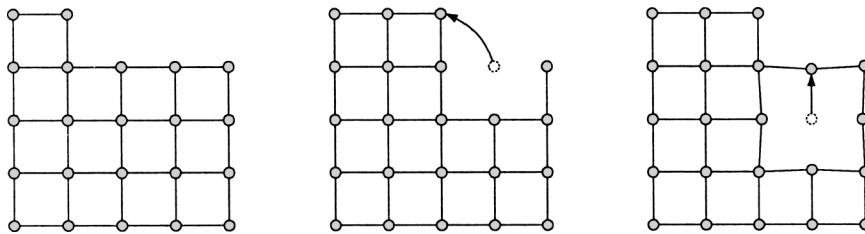


Fig. A.31 Schottky mechanism for vacancy formation. Source: Ref A.5 as published in Ref A.1

Solute atoms of a second metal can be present as impurities or added as intentional alloying elements. These solute atoms can substitute on the crystalline lattice for solvent atoms and form substitutional point defects, or they can be located in the interstitial locations between the atoms of the crystalline lattice to form interstitial defects (Fig. A.32). If the solute impurities are close to the same diameter as the solvent atoms, they will substitute for solvent atoms to form substitutional defects. Small atoms that can fit in between the larger solvent atoms of a crystalline structure are called interstitials. To form interstitial defects, the atomic diameter of the impurity has to be significantly smaller than the solvent atom diameter. Therefore, only atoms with very small diameters, such as carbon, nitrogen, hydrogen, and boron, can form interstitial defects. If the foreign atoms cause harmful or undesirable effects, they are called impurities, while if they are helpful, they are referred to as alloying elements.

Point defects influence solid-state processes such as diffusion, dislocation motion, phase transformations, and electrical conductivity. Point defects typically strengthen a metal and decrease its ductility by impeding the motion of dislocations. Point defects also decrease electrical conductivity, because they interfere with the flow of electrons through the lattice.

Line Defects. One of the most important defects is the line or edge dislocation. The existence of line defects in crystals, called dislocations, provides the mechanism that allows mechanical deformation. A crystal-line metal without dislocations, although extremely strong, would also be extremely brittle and practically useless as an engineering material. Thus, dislocations play a central role in the determination of such important properties as strength and ductility. In fact, virtually all mechanical properties of metals are to a significant extent controlled by the behavior of line imperfections.

As shown in Fig. A.33, an edge dislocation can be visualized as resulting from the insertion of an extra half-plane of atoms above (or below) the

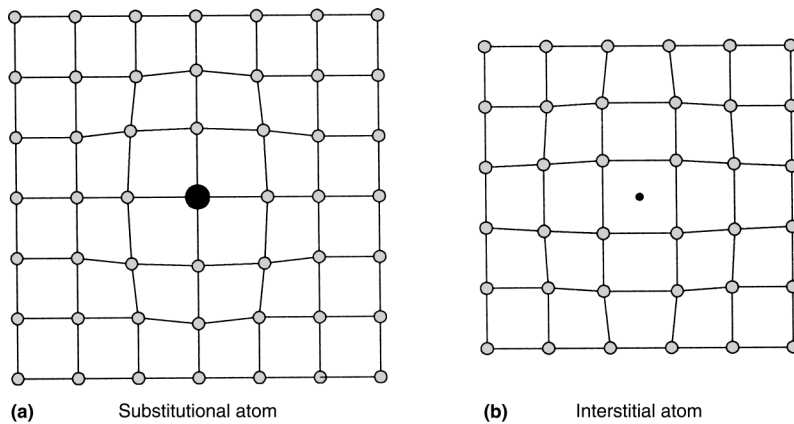


Fig. A.32 Foreign atom point defects. Source: Ref A.5 as published in Ref A.1

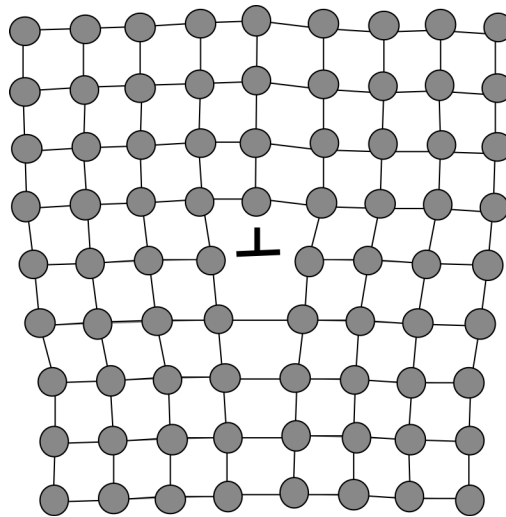


Fig. A.33 Line dislocation. Source: Ref A.1

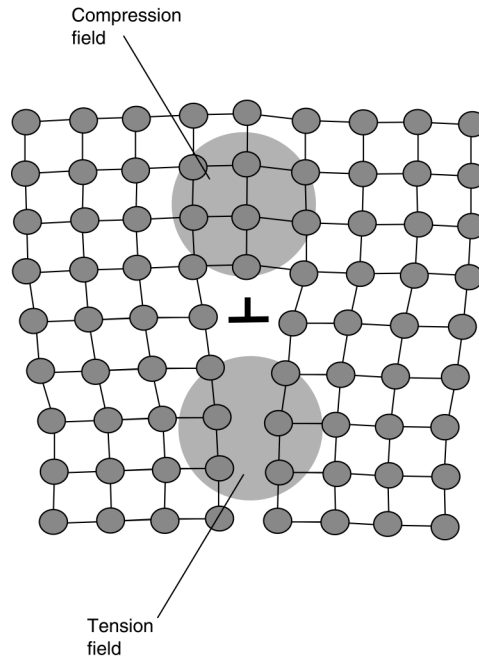


Fig. A.34 Stress field around line dislocation. Source: Ref A.1

dislocation line. By definition, the dislocation shown in Fig. A.33 is a positive dislocation. A negative dislocation has the extra half-plane below the dislocation line. An edge dislocation creates a zone of elastic deformation around the dislocation (Fig. A.34). The lattice below the dislocation is in a state of tension, while above the dislocation there is a compressive stress field. In the lattice below a dislocation, interstitial atoms usually cluster in regions where the tensile stresses help make more room for them.

A quantitative description of dislocations is given by the Burgers vector, b , illustrated in Fig. A.35. This vector is defined using what is called the Burgers circuit, which is an atom-to-atom path that makes a closed loop in a dislocation-free part of the crystal lattice. Now, if the same Burgers circuit is made to encircle a dislocation, the loop does not close. The vector needed to close the loop (the vector from the end of the Burgers circuit to its starting point) is the Burgers vector, b , describing the dislocation. The displacement vector between the two parts of the crystal is denoted by u , and the axis of the dislocation is t . For an edge dislocation, the Burgers vector, b , is perpendicular to the axis of the dislocation, t ($b \perp t$), and parallel to the displacement vector, u ($b \parallel u$).

The other important type of line dislocation is the screw dislocation (Fig. A.36). The term *screw dislocation* is used because of the spiral surface formed by the atomic planes around the screw dislocation line. When a

Burgers circuit is used to determine the Burgers vector of a screw dislocation, the vector is found to be parallel to the dislocation line rather than perpendicular to it, as in the case of an edge dislocation. A screw dislocation is somewhat like a spiral ramp with an imperfection line running down its axis. In a screw dislocation, the Burgers vector, b , is parallel to both the axis of the dislocation, t , and the displacement vector, u ; that is, $(b \parallel t \parallel u)$.

An important characteristic of a dislocation is that it cannot end inside the crystal; it must end at a surface such as a grain boundary or at a surface of the crystal. It is possible for a dislocation to change its character inside the crystal, as shown in the mixed dislocation for an aluminum alloy in Fig. A.37. Here, an edge dislocation is converted to a screw dislocation; in this

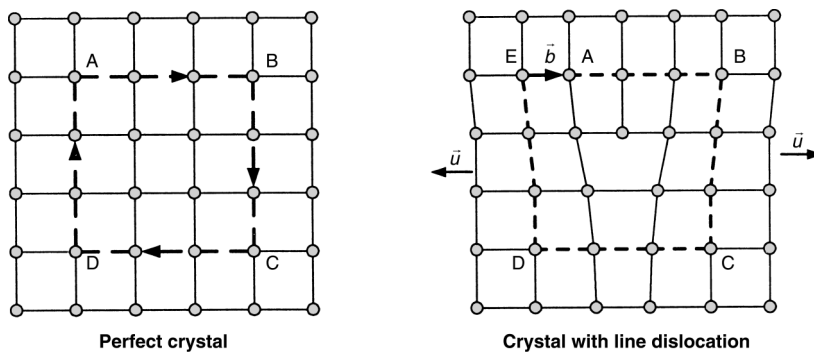


Fig. A.35 Burgers circuit and vector for line dislocation. Source: Ref A.5 as published in Ref A.1

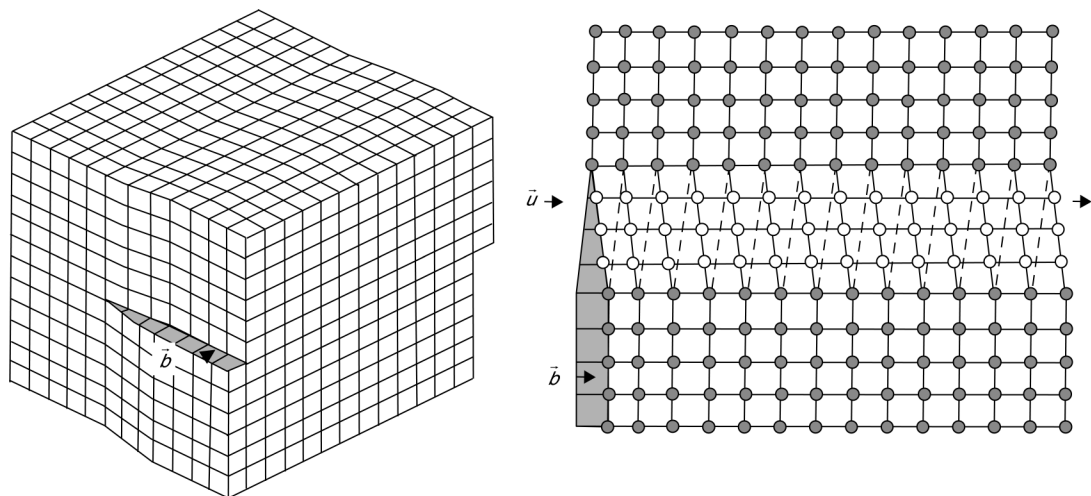


Fig. A.36 Screw dislocation. Source: Ref A.1

case, the screw dislocation is shown ending at the surface of the crystal. Dislocations will also form closed loops within a crystal, changing from an edge to a screw and then back to another edge and finally back to a screw to enclose the loop. The material within the loop is visualized as having slipped on the specified slip plane relative to the material around it.

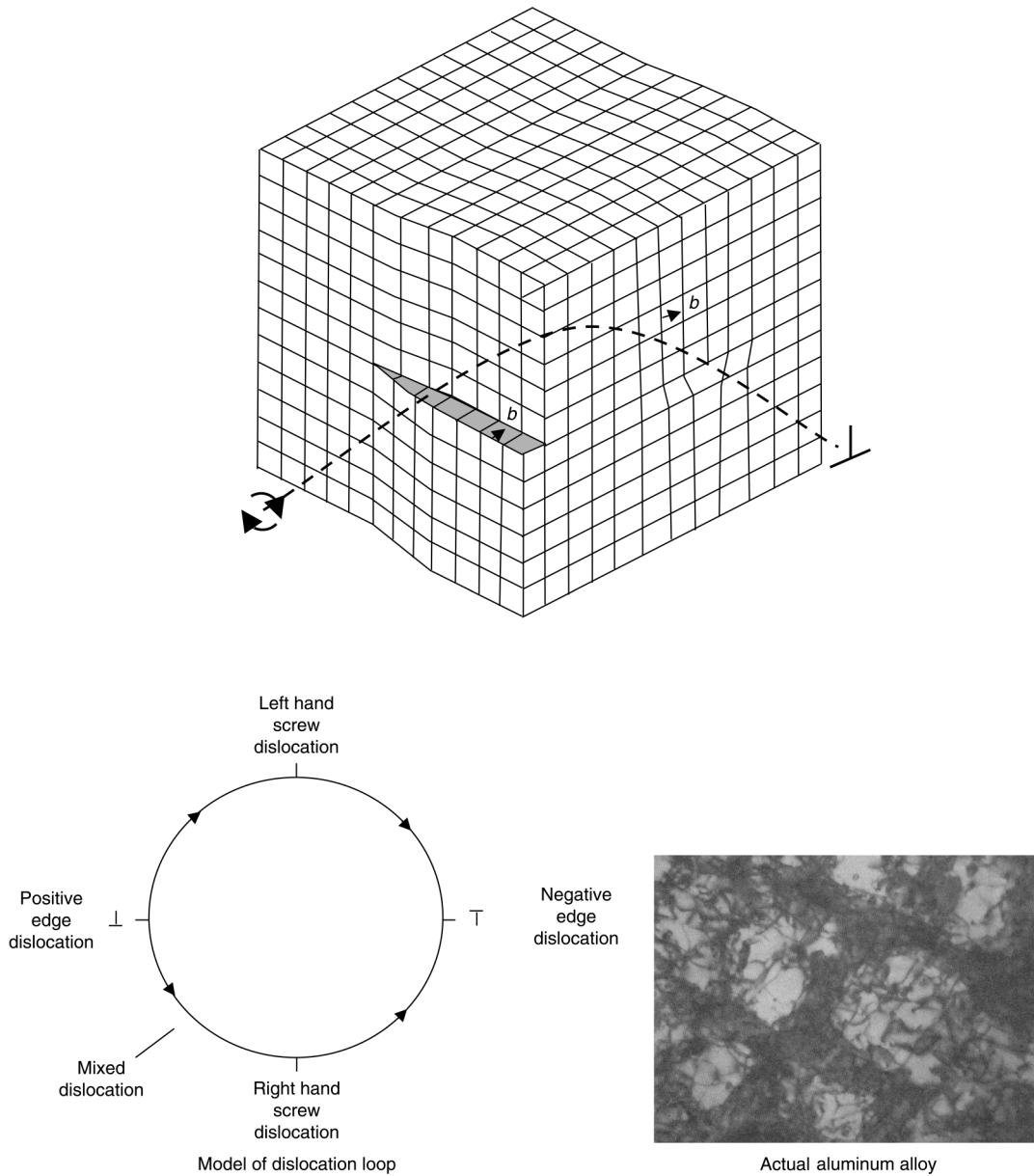


Fig. A.37 Combination screw and line dislocations. Source: Ref A.1

A.9 Plastic Deformation

When a mechanical shear load is applied to a metal, it deforms under the applied stress, as shown schematically in Fig. A.38. If the load is small, the bonds between the atoms will be stretched but will return to their normal lattice positions when the load is removed; this is elastic deformation. However, if a ductile metal is stretched beyond the elastic capability of the bonds, when the load is removed it will not return to its original shape. It is then said to have undergone plastic deformation. On the other hand, if the material is brittle rather than ductile, when the elastic stretching of the bonds is exceeded, it immediately fails with little or no evidence of plastic deformation. This is the type of failure that is normally encountered in covalently and ionically bonded solids, such as glasses and crystalline ceramics. The question becomes: Why do metals exhibit moderate-to-large amounts of plastic deformation, while other materials, such as glasses and ceramics, exhibit almost no ductility and fail in a brittle manner?

The nondirectional metallic bond allows metals to deform by shear as illustrated in Fig. A.39. For the atoms in the upper plane to slide over those in the lower plane, strong interatomic forces must be overcome by the applied shear stress. When the atoms in the upper plane have been displaced by one-half of their transit distance, the crystal energy is at a maximum and then falls once they reach their new equilibrium positions. The shear stress required to cause slip is initially zero when the two planes

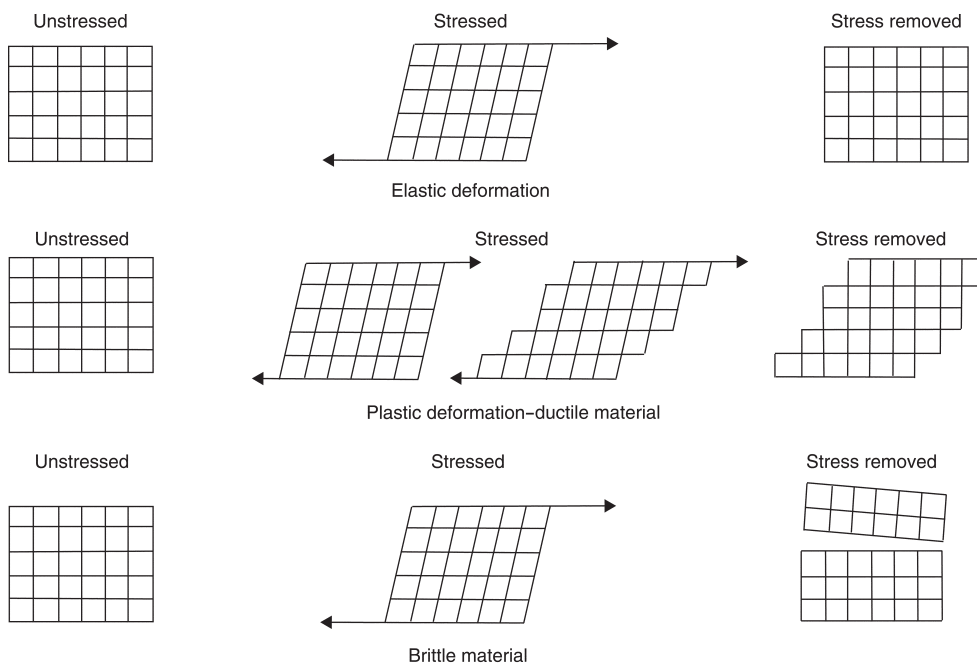


Fig. A.38 Material behavior under stress. Source: Ref A.1

are in coincidence and when the atoms of the top plane are midway between those of the bottom plane, because this is a symmetry position. Between these positions, each atom is attracted to its nearest atom of the other row, so that the shearing stress is a periodic function of the displacement. This shear, or slip, takes the path of least resistance and thus occurs along the close-packed planes in close-packed directions. Atomic bonds are broken and then re-established as the metallic ions move past one another. This is much more difficult for covalently and ionically bonded solids. In the covalent bond, the bonds between two atoms are well established and do not want to be broken. Remember that covalent bonds are both strong and highly directional, while metallic ions share their valence electrons, allowing freer movement through the electron cloud. The problem with ionic bonds is that one ion is positive and the other is negative. During any type of shear mechanism, when two positively charged ions, or two negatively charged ions, approach each other too closely, a strong electrical repulsive force will develop between the two and resist plastic movement.

During tensile testing of a single crystal, shown schematically in Fig. A.40, an applied stress will be reached when the shear stress, resolved onto a slip plane in a slip direction, attains a critical value so that dislocations on that slip plane slip or glide. If the normal, n , of the slip plane lies at an

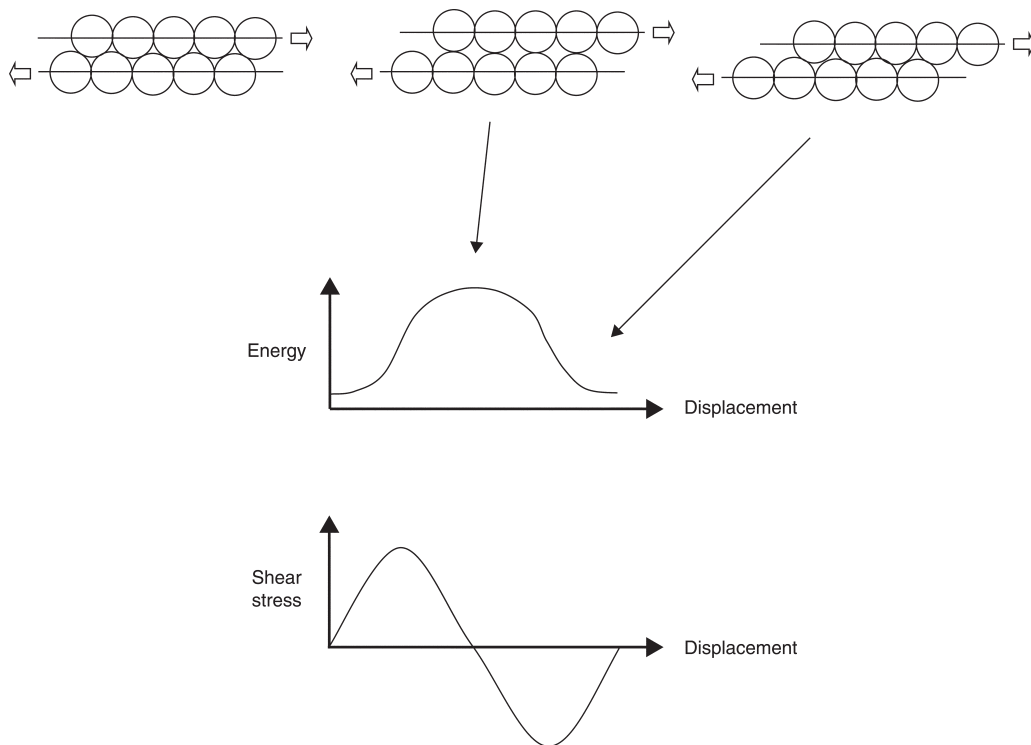


Fig. A.39 Planar slip. Source: Ref A.1

angle, ϕ , to the tensile axis, its area will be $A/\cos \phi$. Similarly, if the slip plane lies at an angle, λ , to the tensile axis, the component of the axial force, P , acting on the slip direction will be $P \cos \lambda$. The resolved shear stress, τ_r , is then given by:

$$\tau_r = \frac{P \cos \lambda}{(A / \cos \phi)} = \sigma \cos \phi \cos \lambda \quad (\text{Eq A.26})$$

For a given metal, the value of τ at which slip occurs is usually found to be a constant, known as the critical resolved shear stress, τ_c . This relationship is known as Schmid's law, and the quantity $\cos \phi \cos \lambda$ is called the Schmid factor. Because the shear stress at which slip occurs is the yield stress, σ_y , it follows that:

$$\tau_c = \sigma_y \cos \phi \cos \lambda \quad (\text{Eq A.27})$$

However, most metals used in industry are polycrystalline, not single crystals. Under an applied axial load, the Schmid factor will be different for each grain. For randomly oriented grains, the average value of the Schmid factor is $\sim 1/3$, which is referred to as the Taylor factor. It then follows that the yield strength should have a value of approximately $3\tau_c$.

Dislocations and Plastic Flow. From our knowledge of the metallic bond, it is possible to derive a theoretical value for the stress required to

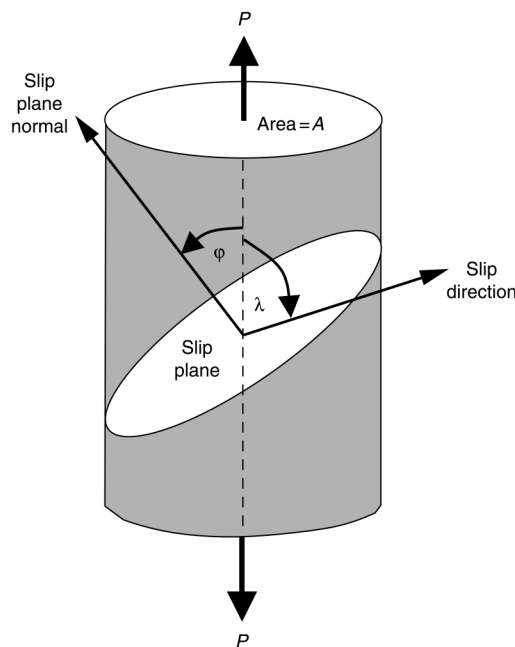


Fig. A.40 Tensile test of single crystal. Source: Ref A.1

produce slip by the simultaneous movement of atoms along a plane in a metallic crystal. However, the strength actually obtained experimentally on single crystals is only approximately one-thousandth (1/1000) of the theoretical value, assuming simultaneous slip by all atoms on the plane. Obviously, slip does not occur by the simple simultaneous block movement of one layer of atoms sliding over another, as previously shown in Fig. A.39. Nor does such a simple interpretation of slip explain work hardening that takes place during mechanical deformation. Earlier theories that sought to explain slip by the simultaneous gliding of a complete block of atoms over another have now been discarded, and the modern concept is that slip occurs by the step-by-step movement of dislocations through the crystal.

When force is applied such that it shears the upper portion of the crystal to the right, as shown in Fig. A.41, the plane of atoms above the dislocation can easily establish bonds with the lower plane of atoms to its right, with the result that the dislocation moves one lattice spacing at a time. Note that only single bonds are being broken at any one time, rather than the whole row, as shown in Fig. A.39. The atomic distribution is again similar to the initial configuration and so the slipping of atom planes can be repeated. The movement is much like that of advancing a carpet along a floor by using a wrinkle that is easily propagated down its length. This stress required to cause plastic deformation is orders of magnitude less when dislocations are present than in a dislocation-free, perfect crystalline structure. If a large number of dislocations move in succession along the same slip plane, the accumulated deformation becomes visible, resulting in macroscopic plastic deformation. Slip can take place by both edge and screw dislocations, as shown in Fig. A.42. Note that although the mechanisms are different, the unit slip produced by both is the same.

Dislocations do not move with the same degree of ease on all crystallographic planes nor in all crystallographic directions. Ordinarily, there are preferred planes, and in these planes, there are specific directions along which dislocation motion can occur. These planes are called slip planes, and the direction of movement is known as the slip direction. The combination of a slip plane and a slip direction forms a slip system. For a

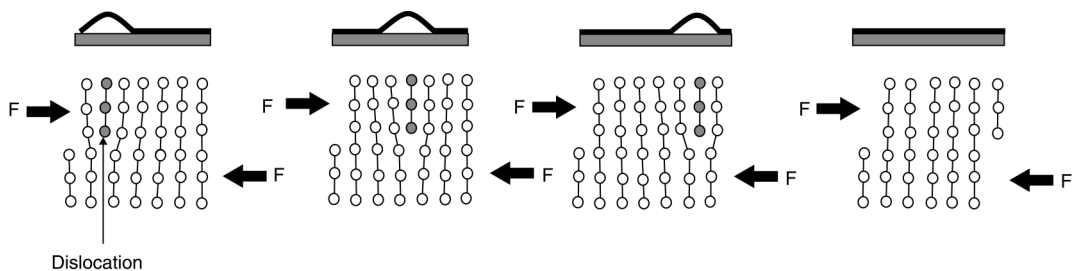


Fig. A.41 Line dislocation movement. Source: Ref A.1

particular crystal structure, the slip plane is that plane having the most dense atomic packing; that is, it has the greatest planar density. The slip direction corresponds to the direction, in this plane, that is most closely packed with atoms, that is, has the highest linear density. Because plastic deformation takes place by slip, or sliding, on the close-packed planes, the greater the number of slip systems available, the greater the capacity for plastic deformation. The major slip systems for the common metallic crystalline systems are summarized in Table A.3.

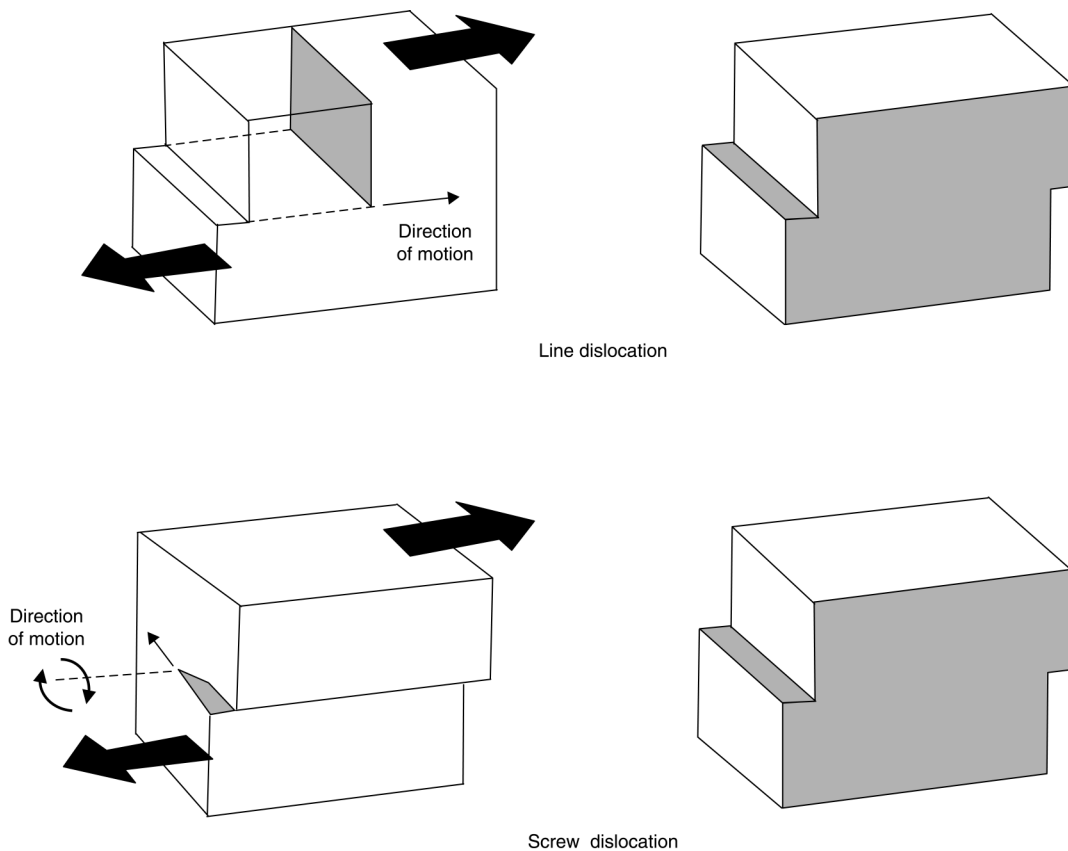


Fig. A.42 Displacements caused by line and screw dislocations. Source: Ref A.1

Table A.3 Major slip systems for common crystal systems

Crystal system(a)		Slip planes		Slip directions		No. of slip systems
Notation	Notation	Number	Notation	Number	Number	Number
bcc	{110}	6	<111>	2	12	12
fcc	{111}	4	<110>	3	12	12
hcp	(0001)	1	[11 $\bar{2}$ 0]	3	3	3

(a) bcc, body-centered cubic; fcc, face-centered cubic; hcp, hexagonal close-packed. Source: Ref A.5 as published in Ref A.1

all temperatures, climb is practically nonexistent at temperatures below approximately $0.4 T_m$, where T_m is the absolute melting point. However, climb becomes an important deformation mechanism when the metal is subjected to stresses at temperatures exceeding approximately $0.4 T_m$.

The dislocation density for crystals is approximately 10^8 cm^{-2} , corresponding to an average distance between dislocations of a few thousand atoms. If each dislocation produces only one unit of slip, this relatively small number of dislocations could not produce large-scale plastic deformation. Thus, a large number of dislocations must be present to produce macroscopic slip. The Frank-Read spiral mechanism (Fig. A.44) explains how dislocations can multiply and increase their effectiveness a thousand-fold. If a dislocation line becomes immobilized and is pinned at its ends, it will tend to bow out under the influence of an applied shear stress. Eventually, the loop becomes circular and then starts closing in on itself at the ends. This allows the formation of a new loop that again bows out under the influence of a shear stress. This process is repeated over and over again, each time generating a new dislocation loop.

Dislocations are influenced by the presence of other dislocations and interact with each other, as shown for a number of different interactions in Fig. A.45. Dislocations with Burgers vectors of the same sign will repel each other, while dislocations of opposite signs will attract each other and, if they meet, annihilate each other. If the two dislocations of opposite signs are not on the same slip plane, they will merge to form a row of vacancies. These types of interactions occur because they reduce the internal energy of the system. When a dislocation becomes pinned by an obstacle

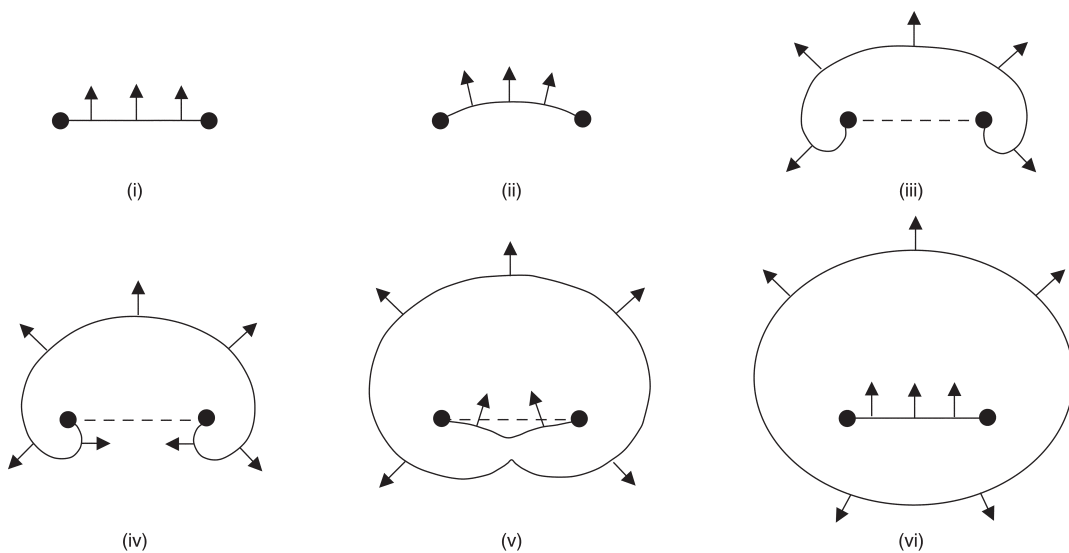


Fig. A.44 Frank-Read mechanism for dislocation multiplication. Source: Ref A.1

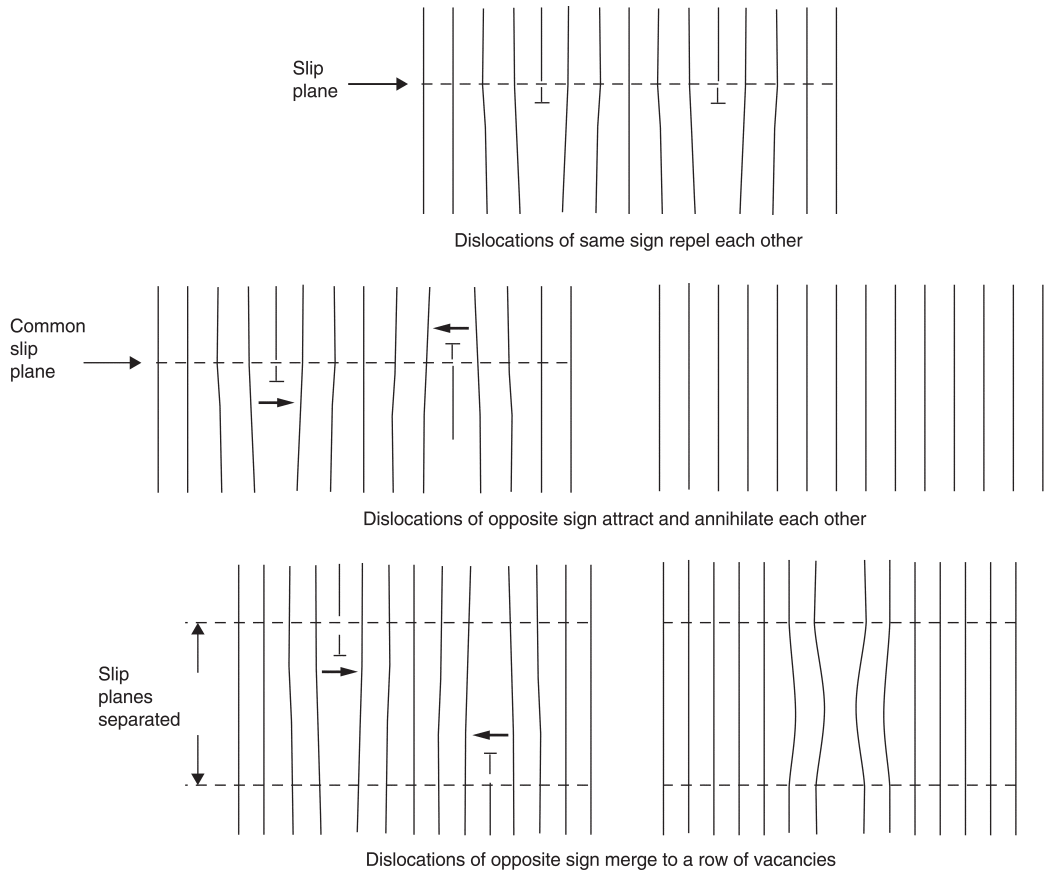


Fig. A.45 Examples of dislocation interactions. Source: Ref A.1

and is immobile, it is termed a sessile dislocation. A dislocation that is not impeded and can move through the lattice is called a glissile dislocation.

If dislocations could only move by gliding on a single slip plane, they would soon be impeded by obstacles and their motion would be restrained. However, screw dislocations can bypass obstacles on their slip plane by cross slipping onto an alternate plane (Fig. A.46). While line dislocations cannot cross slip, they can often convert themselves into screw dislocations while they cross slip. Vacancy diffusion also contributes significantly to high-temperature creep.

Work Hardening. While slip is required to facilitate plastic deformation, and therefore allow a metal to be formed into useful shapes, strengthening metals requires increasing the number of barriers to slip and reducing the ability to plastically deform. Increasing the interference to slip, and increasing the strength, can be accomplished by methods such as plastic deformation. As a metal is plastically deformed, new dislocations

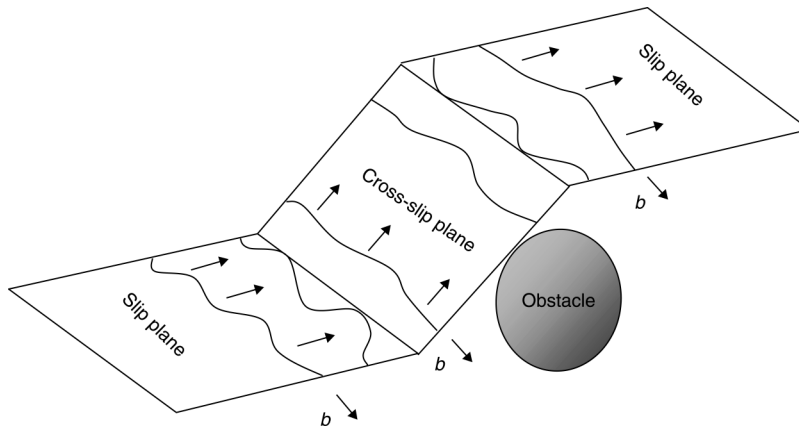


Fig. A.46 Cross slip of screw dislocation. Source: Ref A.1

are created, so that the dislocation density becomes higher and higher. In addition to multiplying, the dislocations become entangled and impede each others' motion. The result is increasing resistance to plastic deformation with increasing dislocation density. The number of dislocations is defined by the dislocation density, ρ , which is the length of dislocations per unit volume of material. Therefore, the units of ρ are cm/cm^3 or cm^{-2} . The dislocation density of an annealed metal usually varies between approximately 10^6 to 10^7 cm^{-2} , while that for a cold worked metal may run as high as 10^8 to 10^{11} cm^{-2} .

This continual increase in resistance to plastic deformation is known as work hardening, cold working, or strain hardening. Work hardening results in a simultaneous increase in strength and a decrease in ductility. Because the work-hardened condition increases the stored energy in the metal and is thermodynamically unstable, the deformed metal will try to return to a state of lower energy. This generally cannot be accomplished at room temperature. Elevated temperatures, in the range of $\frac{1}{2}$ to $\frac{3}{4}$ of the absolute melting point, are necessary to allow mechanisms, such as diffusion, to restore the lower-energy state. The process of heating a work-hardened metal to restore its original strength and ductility is called annealing. Metals undergoing forming operations often require intermediate anneals to restore enough ductility to continue the forming operation. Approximately 5% of the energy of deformation is retained internally as dislocations when a metal is plastically deformed, while the rest is dissipated as heat.

A.10 Surface or Planar Defects

Surface, or planar, defects occur whenever the crystalline structure of a metal is discontinuous across a plane. Surface defects extend in two directions over a relatively large surface with a thickness of only one or two

lattice parameters. Grain boundaries and phase boundaries are independent of crystal structure, while coherent phase boundaries, twin boundaries, and stacking faults all depend on the crystalline structure.

A.10.1 Grain Boundaries

The most important surface defect is the grain boundary. Most metals are polycrystalline and consist of many small crystallites called grains. The interfaces between these grains are called grain boundaries and are only

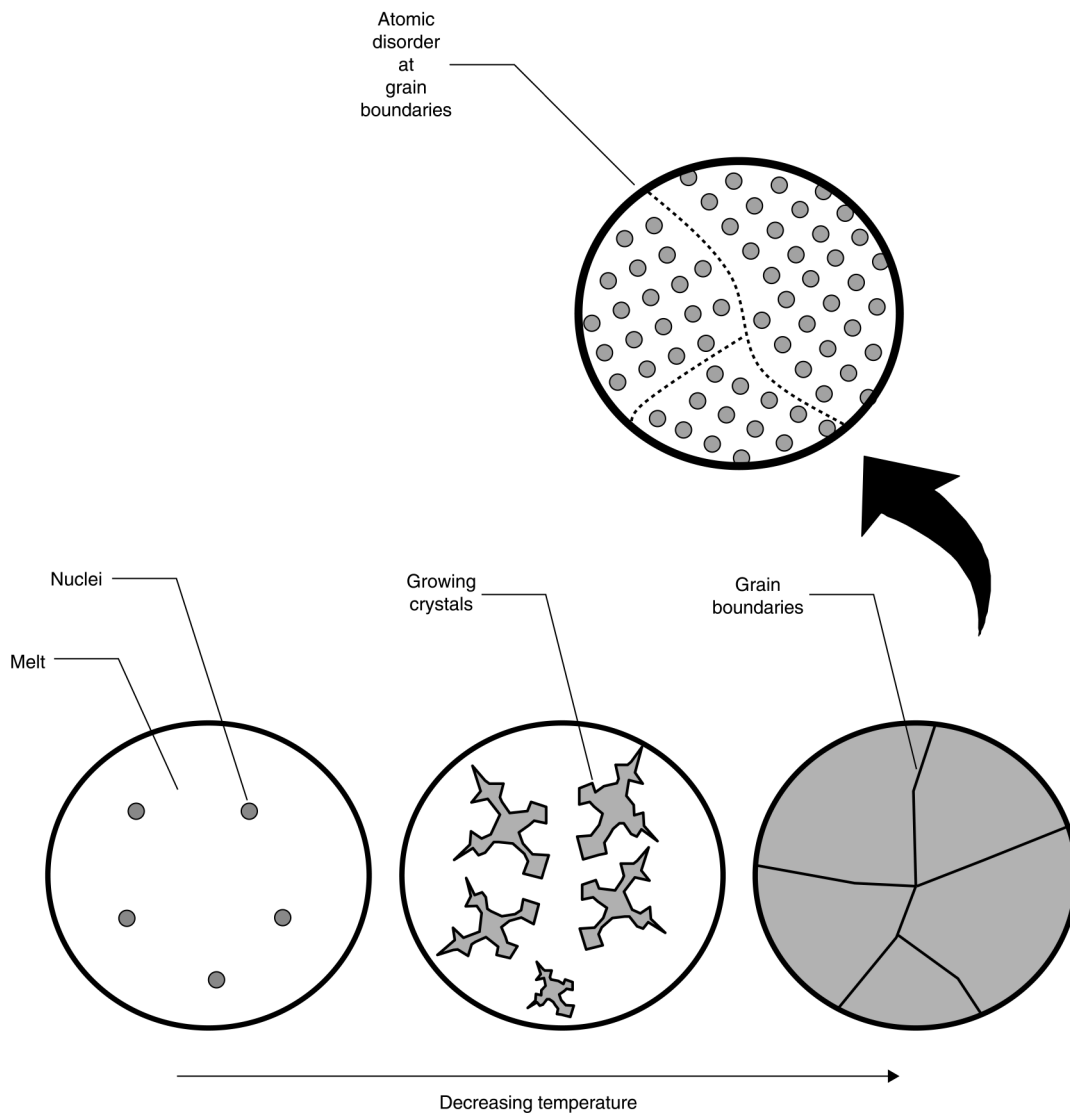


Fig. A.47 Solidification sequence for a metal. Source: Ref A.1

one or two atoms thick, because the system wants to reduce the free energy as much as possible. Atoms within the grain boundaries are highly strained and distorted; therefore, grain boundaries are high-energy sites. The average diameter of the individual grains within a polycrystalline metal defines the metal grain size. Grain boundaries are a result of the solidification process and occur as a result of the misorientation of the grains as they are frozen into position (Fig. A.47).

Small-angle grain boundaries occur when the misorientation between grains is small, usually less than 5° . These small-angle misorientations can be represented by a row of somewhat parallel edge dislocations, as shown for the low-angle tilt boundary in Fig. A.48. The regions between the dislocations consist of an almost perfect fit and have low strain, while regions at the dislocation cores have poor fit and are high-strain regions. The regions surrounded by low-angle grain boundaries are called subgrains or subcrystals and are essentially free of dislocations. The spacing between dislocations, D , is:

$$D = \frac{b}{\sin \theta} \cong \frac{b}{\theta} \quad (\text{Eq A.28})$$

where θ is the angular misorientation across the boundary. A gross grid of two screw dislocations can also form a low-angle grain boundary, in this instance it is called a low-angle twist boundary.

If the misorientation is greater than approximately 10 to 15° , then high-angle grain boundaries will form, as previously illustrated in Fig. A.48. Because high-angle grain boundaries result in a less ordered arrangement of the atoms with large areas of misfit and a relatively more open structure,

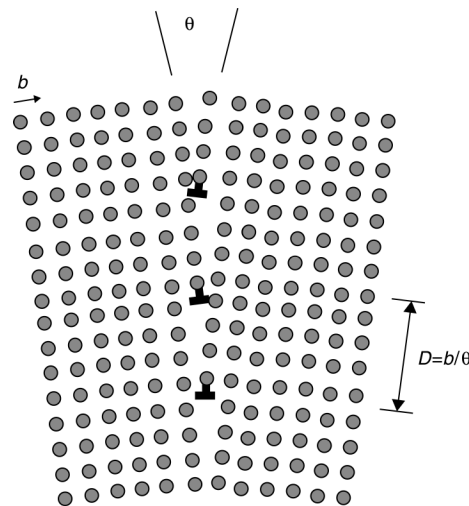


Fig. A.48 Low-angle tilt boundary. Source: Ref A.1

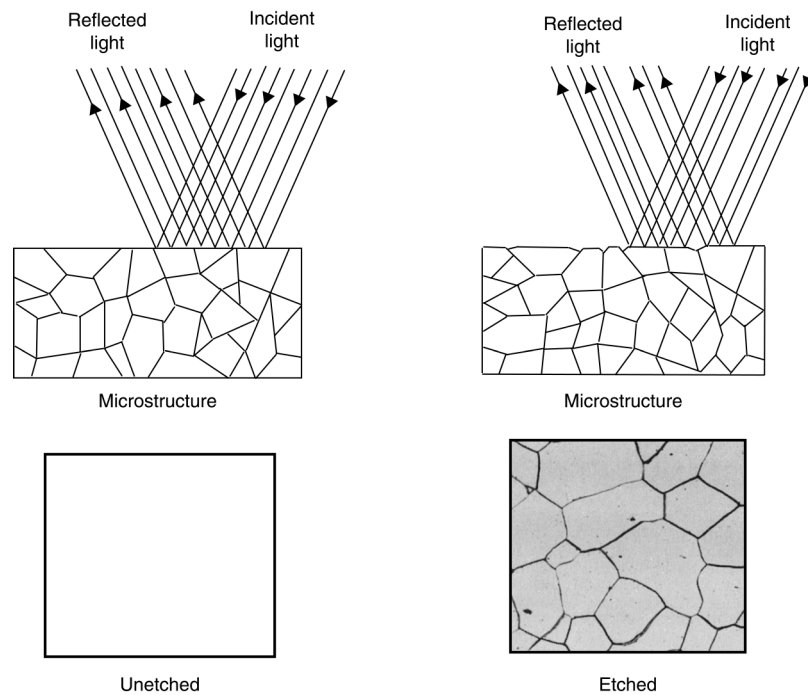


Fig. A.49 Metallography of unetched and etched samples. Source: Ref A.1

the atoms along the grain boundaries have a higher energy than the atoms within the grain interiors. Thus, grain boundaries are regions with many irregularly placed atoms, dislocations, and voids. Compared with high-angle boundaries, low-angle boundaries have less severe defects, obstruct plastic flow less, and are less susceptible to chemical attack and segregation of alloying constituents. In general, mixed types of grain-boundary defects are common. All grain boundaries are sinks into which vacancies and dislocations can disappear.

Grain boundaries, as well as other microstructural features, are often observed by polishing a metal surface, lightly etching it with an acid, and then examining it with a light microscope at magnification. Grain boundaries become visible when the polished surface is etched with the proper acid, creating a microscopically uneven surface that reflects the light slightly differently (Fig. A.49) than the unetched surface.

A grain boundary tends to minimize its area in order to reduce the internal energy of the system. The driving force for this energy reduction is surface tension, which can be reduced by straightening of the irregular-shaped boundaries. If a grain has less than six boundaries, then each boundary will be concave inward and will be unstable. On the other hand, if a grain has more than six sides, the boundaries will be planar and stable. At high temperatures, for example, during annealing operations at $T > 0.5$

T_m , there is an exponential increase in the mobility of the atoms. Grains with six or more boundaries will tend to grow, while grains with less than six sides will shrink and be consumed by larger grains. Atoms in the shrinking grains will migrate across the boundary interface to join the larger growing grains. The presence of second-phase particles helps to pin the grain boundaries and impede grain growth. At equilibrium (Fig. A.50), all three grain boundaries will have the same surface tension, γ , and all three will have angles $\theta = 120^\circ$. If all of the boundaries meet at 120° , then the shape of the grain will fill all of the available area and is called a tetrakaidecahedron which contains 14 faces, 36 edges, and 24 corners. A stack of six tetrakaidecahedra is shown in Fig. A.51.

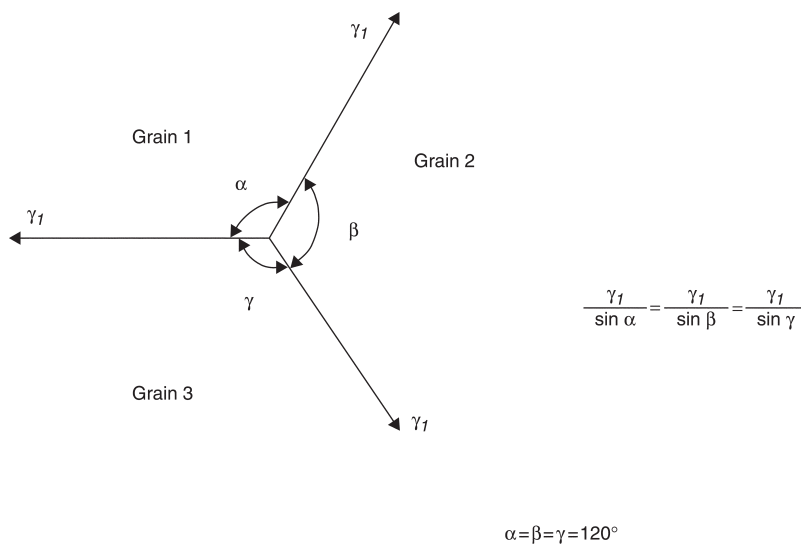


Fig. A.50 Grain boundaries in equilibrium. Source: Ref A.6 as published in Ref A.1

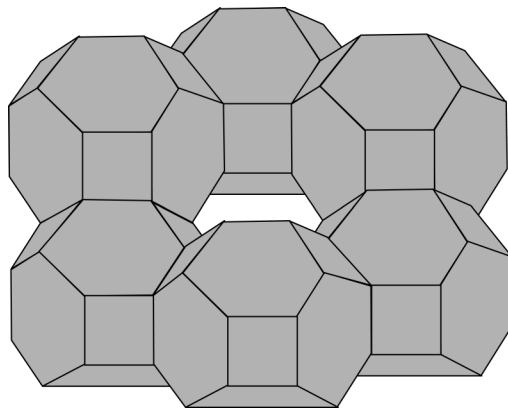


Fig. A.51 Stack of tetrakaidecahedra. Source: Ref A.6 as published in Ref A.1

Grain boundaries are preferential regions for accumulation and segregation of many types of impurities. Weakening or embrittlement can also occur by preferential phase precipitation or absorption of environmental species, such as hydrogen or oxygen, in the grain boundaries. At room temperature, the grain boundaries are usually stronger than the grain interiors, and failure usually occurs through the grain themselves (transgranular). However, at high temperatures, the grain boundaries typically become the weak link, and failure occurs through the grain boundaries (intergranular). Thus, a coarse grain structure is desirable for high-temperature applications, while fine grains and finely divided phase regions are preferred for most room- and low-temperature applications.

Polycrystalline Metals. In the single-crystal tensile stress where the critical resolved shear stress was determined (Fig. A.40), the slip planes were not restricted by the presence of other grains, and slip occurs as in the left-hand portion of Fig. A.52. However, in polycrystalline metals, the orientation of the slip planes in adjoining grains is seldom aligned, and the slip plane must change direction when traveling from one grain to

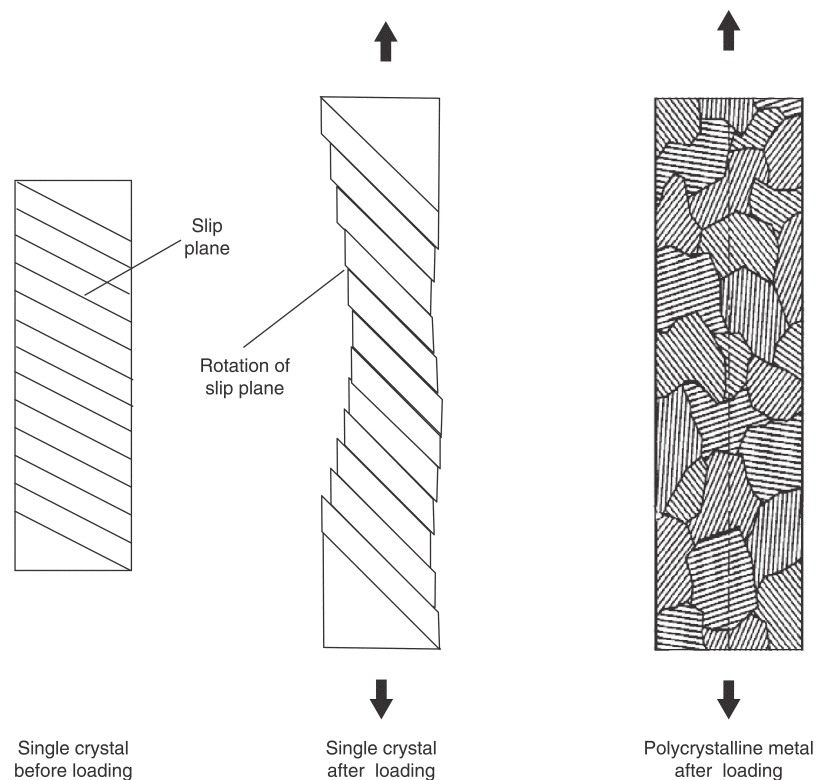


Fig. A.52 Tension loading of single and polycrystalline metals. Source: Ref A.1

another. Reducing the grain size produces more changes in direction of the slip path and also lengthens it, making slip more difficult; therefore, grain boundaries are effective obstacles to slip. In addition, dislocations cannot cross the high-energy grain boundaries; instead they are blocked and pile up at the boundaries (Fig. A.53). Decreasing the grain size is effective in both increasing strength and also increasing ductility, and, as such, is one of the most effective strengthening mechanisms. Fracture resistance also generally improves with reductions in grain size, because the cracks formed during deformation, which are the precursors to those causing fracture, are limited in size to the grain diameter. The yield strength of many metals and their alloys has been found to vary with grain size according to the Hall-Petch relationship:

$$\sigma_y = \sigma_0 + k_y d^{-1/2} \quad (\text{Eq A.29})$$

where k_y is the Hall-Petch coefficient, a material constant; d is the grain diameter; and σ_0 is the yield strength of an imaginary polycrystalline metal having an infinite grain size.

The Hall-Petch relationships for a number of metals are shown in Fig. A.54. The value of the Hall-Petch coefficient varies widely for different metals, and grain size refinement is more efficient for some metals than others. For example, grain size refinement significantly increases the yield strength of low-carbon steels (up to 275 MPa, or 40 ksi), while it provides only approximately a 60 MPa (9 ksi) increase for a typical aluminum alloy.

Because the grain size of a metal or alloy has important effects on the structural properties, a number of methods have been developed to measure the grain size of a sample. In all methods, some form of microexamination is used in which a small sample is mounted, polished, and then etched to reveal the grain structure. The most direct method is then to count the

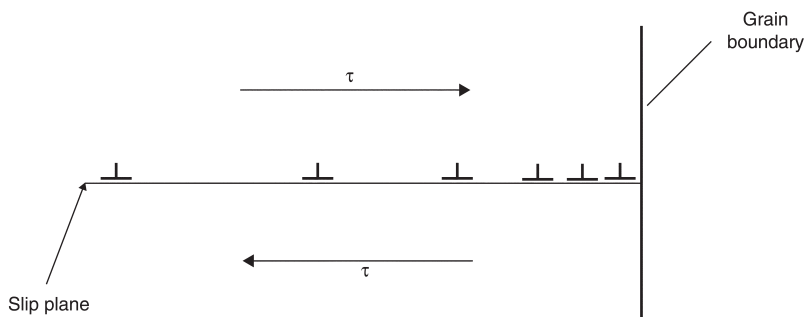


Fig. A.53 Dislocation pile-up at grain boundary. Source: Ref A.1

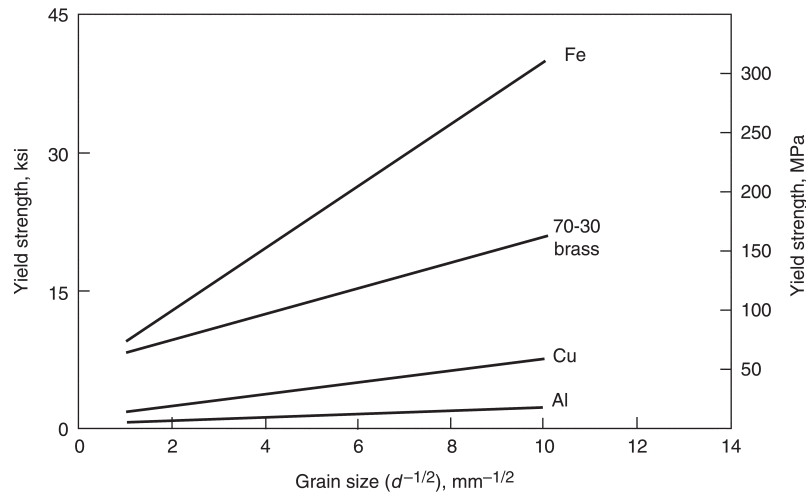


Fig. A.54 Hall-Petch relationship. Source: Ref A.1

number of grains present in a known area of the sample so the grain size can be expressed as the number of grains/area.

ASTM International has developed standard procedures for determining average grain size. The ASTM grain size number provides a convenient method for communicating grain sizes. For materials with a uniform grain size distribution, the ASTM grain size number is derived from the number of grains/ in.^2 when counted at a magnification of $100\times$. The ASTM index, N , is given by:

$$n = 2^{(N-1)} \quad (\text{Eq A.30})$$

where n is the number of grains/ in.^2 at $100\times$ magnification. To obtain the number of grains per square millimeter at $1\times$, multiply n by 15.50. This can be rewritten as:

$$\log n = (N - 1) \log 2 \quad (\text{Eq A.31})$$

or

$$N = \frac{\log n}{0.3010} + 1 \quad (\text{Eq A.32})$$

A listing of ASTM grain size numbers and the corresponding grain size is given in Table A.4. Note that larger ASTM grain size numbers indicate more grains per unit area and finer, or smaller, grain sizes.

A.10.2 Phase Boundaries

While a grain boundary is an interface between grains of the same composition and same crystalline structure (α/α interface) with different orientations, a phase boundary is one between two different phases (α/β interface) that can have different crystalline structures and/or different compositions. In two-phase alloys, such as copper-zinc brass alloys containing more than 40% Zn, second phases, such as the one shown in Fig. A.55, can form due to the limited solid solubility of zinc in copper.

There are three different types of crystalline interfaces that can develop between two phases (Fig. A.56): coherent, semicoherent, and incoherent. A fully coherent phase boundary (Fig. A.56a, b) occurs when there is perfect atomic matching and the two lattices are continuous across the interface. The interfacial plane will have the same atomic configuration in both planes. Because there is perfect matching at the interface, the

Table A.4 ASTM grain size, $n = 2^{(N-1)}$

Grain size no.	Average number of grains/unit area	
	No./in. ² at 100 \times	No./mm ² at 1 \times
$N = 1$	$n = 1.00$	$n = 15.50$
2	2.00	31.00
3	4.00	62.00
4	8.00	124.00
5	16.00	496.00
6	32.00	992.00
7	64.00	1984.0
8	128.00	3968.0
9	256.00	3968.0
10	512.00	7936.0

Source: Ref A.7 as published in Ref A.1

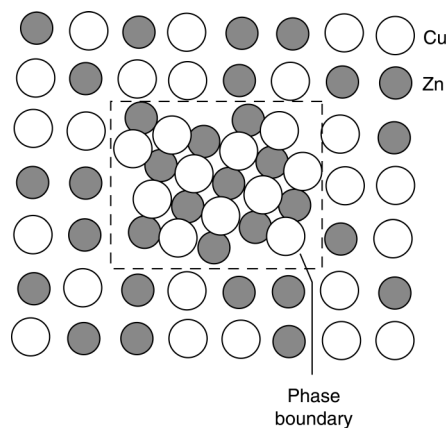


Fig. A.55 Phase boundary in copper-zinc system. Source: Ref A.8 as published in Ref A.1

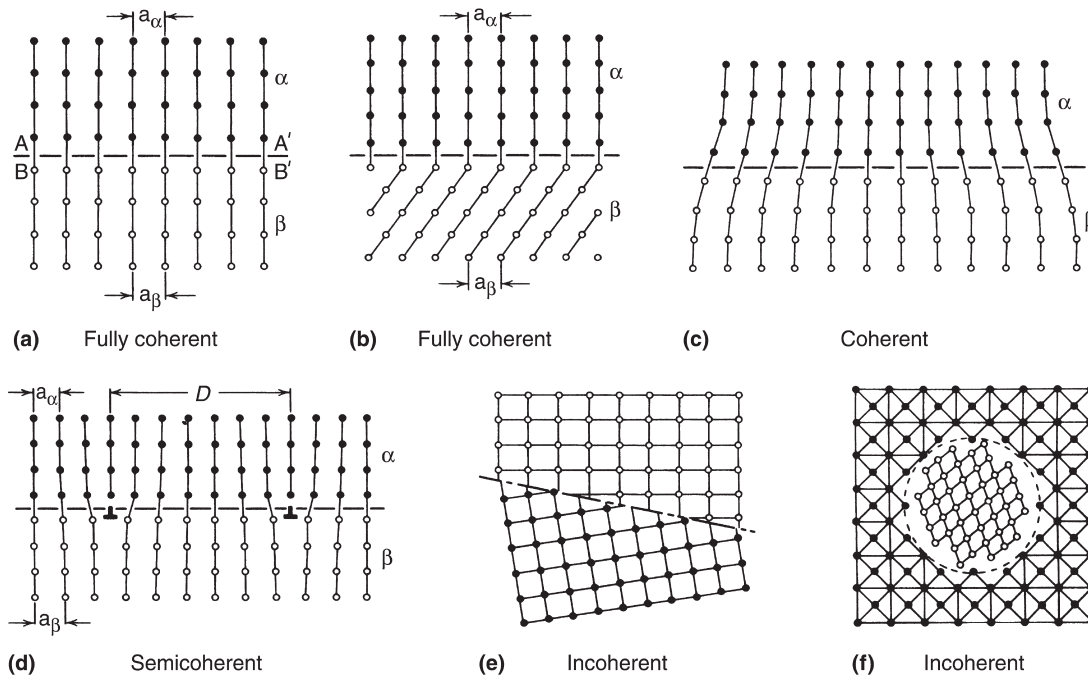


Fig. A.56 Phase boundaries. Source: Ref A.9 as published in Ref A.1

interfacial energy is low, typically up to approximately 200 mJ/m^2 . When the distances between atoms at the interface are not identical (Fig. A.56c), coherency strains start to develop; however, because there is still perfect atomic matching, it is still a coherent phase boundary, only the interfacial energy will be higher than one with no distortion. When the mismatch becomes sufficiently large, dislocations form to accommodate the growing disregistry. The result is called a semicoherent interface (Fig. A.56d) that has an interfacial energy of 200 to 500 mJ/m^2 . Finally, an incoherent interface (Fig. A.56e, f) is an interphase boundary that results when the matrix and precipitate have very different crystal structures, and little or no atomic matching can occur across the interface. The interfacial energy is even greater, reaching values between 500 and 1000 mJ/m^2 . An incoherent boundary is essentially the same as a high-angle grain boundary.

In many instances, second phases have a tendency to form at the grain boundaries. This occurs because they reduce their interfacial energy by occupying a grain boundary; that is, by occupying a grain boundary, part of the interfacial energy is eliminated and the total energy of the system is reduced. Consider the case where two grains of α phase meet with one grain of β phase, as shown in Fig. A.57. The surface energy, γ , will be in equilibrium if:

$$\gamma_{\alpha\alpha} = 2\gamma_{\alpha\beta} \cos \frac{\theta}{2} \quad (\text{Eq A.33})$$

The angle, θ , is called the dihedral angle at the α -to- β interface. If $\gamma_{\alpha\beta} > \frac{1}{2} \gamma_{\alpha\alpha}$, θ will have a finite value; if $\gamma_{\alpha\beta} = \frac{1}{2} \gamma_{\alpha\alpha}$, $\theta = 120^\circ$; and if $\gamma_{\alpha\beta} < \frac{1}{2} \gamma_{\alpha\alpha}$, $\theta > 120^\circ$. However, if $\gamma_{\alpha\alpha} > 2\gamma_{\alpha\beta}$, Eq A.30 cannot be satisfied and no equilibrium will exist. Instead, the β phase will wet the grain boundary and spread out as a thin grain-boundary film. In this case, if the β phase is brittle, or has a low melting point, the mechanical properties of the alloy will be impaired even though the α matrix is strong and tough. This potentially disastrous condition, known as grain-boundary embrittlement, is shown in Fig. A.58.

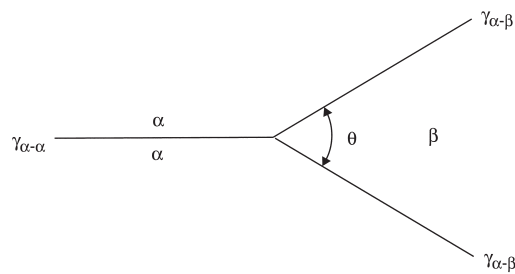


Fig. A.57 Dihedral angle, θ , between two interfaces of differing phases. Source: Ref A.6 as published in Ref A.1

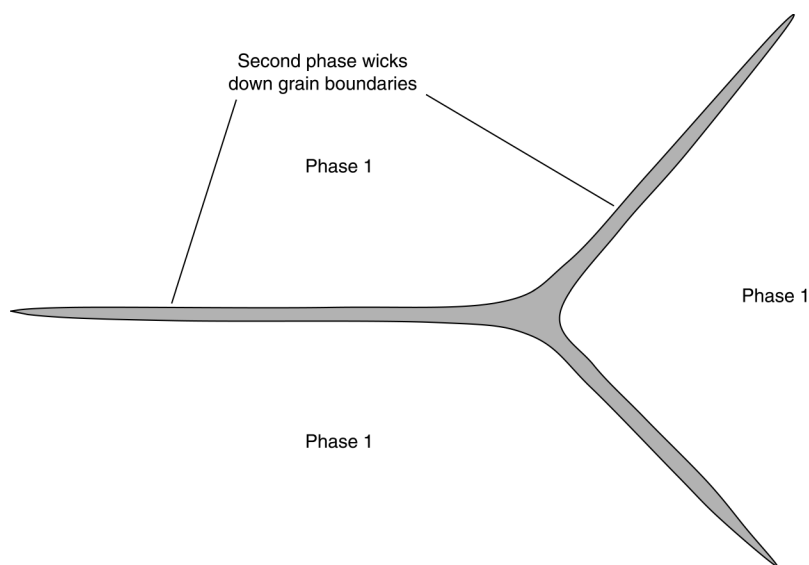


Fig. A.58 Grain-boundary embrittlement. Source: Ref A.2 as published in Ref A.1

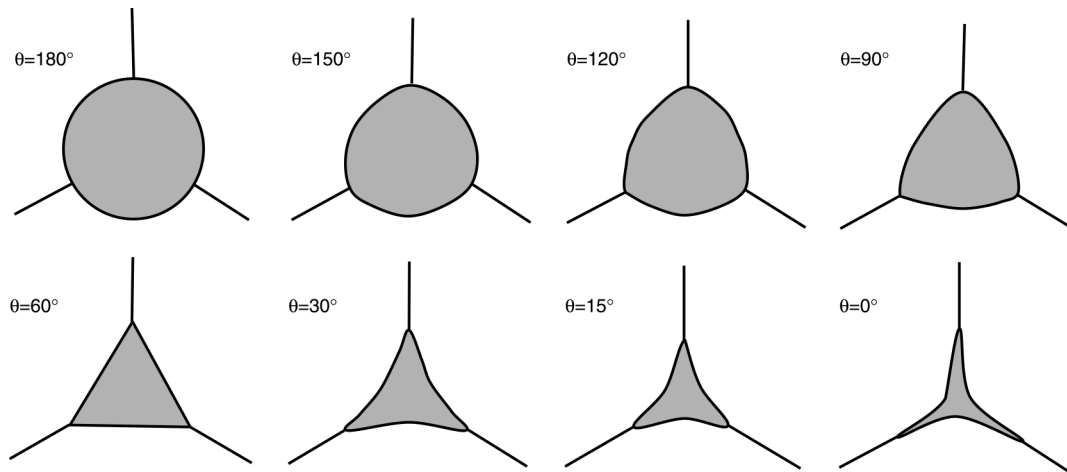


Fig. A.59 Effects of dihedral angle on second-phase shape. Source: Ref A.6 as published in Ref A.1

When the second phase is located at the juncture of three grains, it can form different shapes (Fig. A.59), depending again on the dihedral angle, θ . At small angles, such as $\theta = 0^\circ$, the second phase can penetrate the grain boundaries and possibly affect alloy properties, while at the other extreme ($\theta = 180^\circ$), it will form round particles that should not inhibit alloy performance. Second-phase particles of lead are often added to alloys to improve machinability by forming cleaner chips. Because they form round particles, such as in the case where $\theta = 180^\circ$, they do not adversely affect strength or ductility. There are even some instances where grain-boundary wetting is desirable, such as during liquid phase sintering of carbide cutting tools. Here, a cobalt matrix wets the tungsten carbide particles and binds them together during sintering.

A.10.3 Twinning

Twinning is another mechanism that causes plastic deformation, although it is not nearly as important as dislocation movement. Mechanical twinning is the coordinated movement of large numbers of atoms that deforms a portion of the crystal by an abrupt shearing motion. Atoms on each side of the twinning plane, or habit plane, form a mirror image with those on the other side of the plane (Fig. A.60). Shear stresses along the twin plane cause atoms to move a distance that is proportional to the distance from the twin plane. However, atom motion with respect to one's nearest neighbors is less than one atomic spacing. Twins occur in pairs, such that the change in orientation of the atoms introduced by one twin is restored by the second twin. Twinning occurs on a definite crystallographic plane and in a specific direction that depends on the crystalline structure. Twins

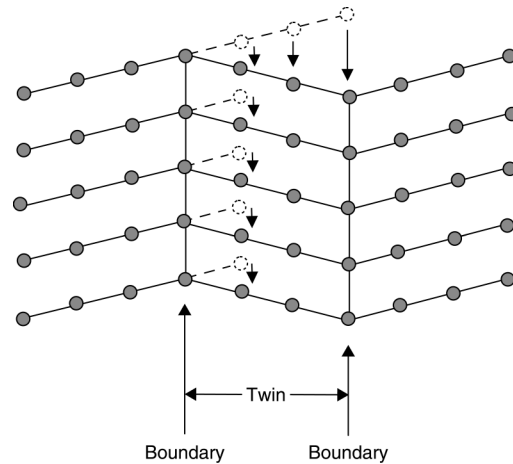


Fig. A.60 Deformation by twinning. Source: Ref A.1

can occur as a result of plastic deformation (deformation twins) or during annealing (annealing twins). Mechanical twinning occurs in bcc and hcp metals, while annealing twins are fairly common in fcc metals.

Mechanical twinning increases the strength because it subdivides the crystal, thereby increasing the number of barriers to dislocation movement. Twinning is not a dominant deformation mode in metals with multiple slip systems, such as fcc structures. Mechanical twinning occurs in metals that have bcc and hcp crystalline structures at low temperatures and at high rates of loading, conditions in which the normal slip process is restricted due to few operable slip systems. The amount of bulk plastic deformation in twinning is small compared to slip. The real importance of twinning is that crystallographic planes are reoriented so that additional slip can take place.

Unlike slip, the shear movements in twinning are only a fraction of the interatomic spacing, and the shear is uniformly distributed over volume rather than localized on a number of distinct planes. Also, there is a difference in orientation of the atoms in the twinned region compared to the untwinned region that constitutes a phase boundary. Twins form suddenly, at a rate approaching the speed of sound, and can produce audible sounds such as “tin cry.” Because the amount of atom movement during twinning is small, the resulting plastic deformation is also small.

A comparison of the slip and twinning mechanisms is shown in Fig. A.61. The differences between the two deformation mechanisms include:

- *Orientation.* In slip, the orientation above and below the slip plane is the same after slip, while in twinning there is an orientation change across the twin plane.

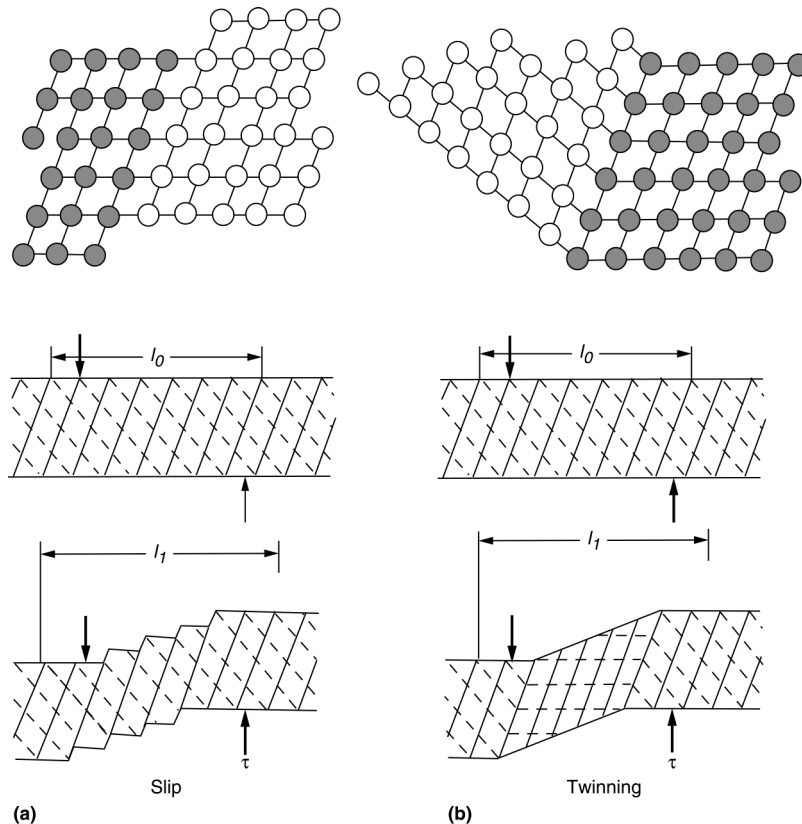


Fig. A.61 Comparison of slip and twinning deformation mechanisms occurring over a length, l , under a shear stress, τ . Source: Ref A.5 as published in Ref A.1

- *Mirror image.* Atoms in the twinned portion of the lattice form a mirror image with the untwinned portion. No such relationship exists in slip.
- *Deformation.* In slip, the deformation is nonhomogeneous because it is concentrated in bands, while the metal adjacent to the bands is largely undeformed. In twinning, the deformation is homogeneous because all of the atoms move cooperatively at the same time.
- *Stress.* In slip, a lower stress is required to initiate it, while a higher stress is required to keep it propagating. In twinning, a high stress is required to initiate, but a very low stress is required for propagation. The shear stress required for twinning is usually higher than that required for slip.

Twin boundaries generally are very flat, appearing as straight lines in micrographs, and are two-dimensional defects of lower energy than high-angle grain boundaries. Therefore, twin boundaries are less effective as

sources and sinks of other defects and are less active in deformation and corrosion than ordinary grain boundaries.

Another type of deformation similar to twinning is kink band formation. Kink band formation usually occurs in hcp metals under compressive loading. It occurs when the applied stress is nearly perpendicular to the principal slip plane, normally the basal plane in hcp metals. In this mechanism, the metal shears by the formation of dislocation arrays that produce buckling along the slip plane direction that shears the metal several degrees away from its previous position. As opposed to twinning, the atomic positions do not form a mirror image after shear displacement.

A.10.4 Stacking Faults

The passage of a total dislocation through a crystalline lattice leaves the perfection of the lattice undisturbed. Each atom is shifted from one normal position in the lattice to an adjacent normal position. However, the energy of the system can sometimes be lowered if a total dislocation splits into a partial dislocation (Fig. A.62). It takes less energy if the total dislocation splits into two partial dislocations that can move in a zigzag path through the valley between atoms, rather than having to climb over an atom. Instead of an atom moving directly from its lattice position to a new position, indicated by the tip of the arrow of the Burgers vector, it can move first to an intermediate vacant site and then again to the final site. Thus, two short jumps are made instead of one longer one, which requires less energy. However, the passage of a partial dislocation leaves behind a planar region of crystalline imperfection.

The planar imperfection produced by the passage of a partial dislocation is called a stacking fault, as illustrated in Fig. A.63. In a fcc structure, the stacking sequence changes from the normal *ABCABC* to *ABAB*, which is the stacking sequence for the hcp structure. Passage of the second partial dislocation restores the normal *ABCABC* stacking sequence. These partial dislocations are often referred to as Schottky partials. The two partial dis-

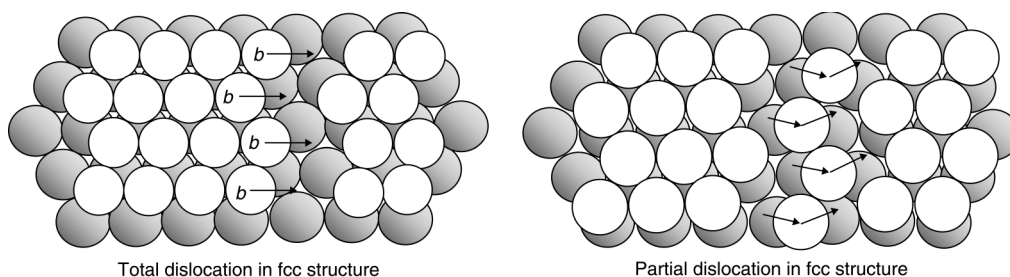


Fig. A.62 Concept of partial dislocation. Source: Ref A.3 as published in Ref A.1

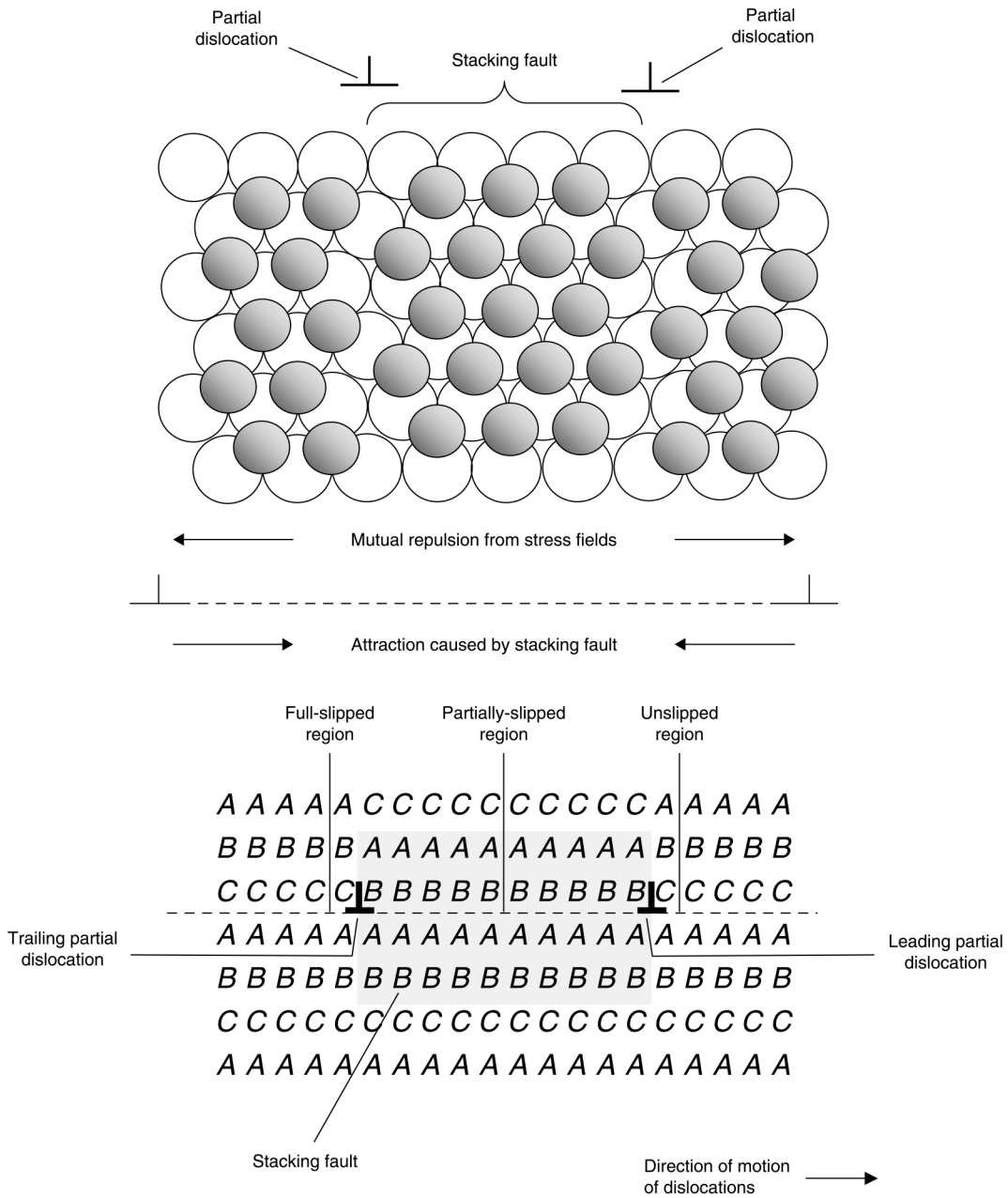


Fig. A.63 Stacking fault and extended dislocation. Source: Ref A.10 and A.3 as published in Ref A.1

locations that are separated by the faulted area are known as an extended dislocation.

The total energy of a perfect lattice is lower than one with a stacking fault. Thus, a stacking fault has an energy associated with it. The difference in energy between a perfect lattice and one with a stacking fault is

known as the stacking fault energy (SFE). Equilibrium occurs between the repulsive energy of the two partials and the surface energy of the fault. The larger the separation between the partial dislocations, the smaller is the repulsive force between them. On the other hand, the surface energy associated with the stacking fault increases with the distance between the two partial dislocations. In general, if the separation between the partial dislocations is small, the metal is said to have a high stacking fault energy. If the separation is large, the metal would have a low stacking fault energy. For example, the separation in aluminum (high SFE) is on the order of an atomic spacing, while that of copper (low SFE) is approximately 12 atomic spacings.

Stacking fault energy plays a role in determining deformation textures in fcc and hcp metals. Stacking faults also influence plastic deformation characteristics. Metals with wide stacking faults (low SFE) strain harden more rapidly and twin more readily during annealing than those with narrow stacking faults (high SFE). Some representative SFEs are given in Table A.5.

A.11 Volume Defects

Volume defects, such as porosity and microcracks, almost always reduce strength and fracture resistance. The reductions can be quite substantial, even when the defects constitute only several volume percent. Shrinkage during solidification can result in microporosity; that is, porosity having diameters on the order of micrometers. In metals, porosity is much more likely to be found in castings than in wrought products. The extensive plastic deformation during the production of wrought metals is usually sufficient to heal or close microporosity.

Powder metallurgy products also frequently contain porosity. Powder metallurgy products are usually produced by blending metal powders, pressing them into a shape, and then sintering them at temperatures just below the melting point. Porosity in powder metallurgy products can be reduced if pressure is used during the sintering process by either hot pressing in a press or hot isostatic pressing under gas pressure.

Table A.5 Approximate stacking fault energies (SFEs)

Metal	SFE, mJ/m ²
Brass	<10
Austenitic Stainless Steel	<10
Silver	20–25
Gold	50–75
Copper	80–90
Nickel	130–200
Aluminum	200–250

Source: Ref A.1

ACKNOWLEDGMENT

The contents of this chapter came from *Elements of Metallurgy and Engineering Alloys* by F.C. Campbell, ASM International, 2008.

REFERENCES

- A.1 F.C. Campbell, *Elements of Metallurgy and Engineering Alloys*, ASM International, 2008
- A.2 V. Singh, *Physical Metallurgy*, Standard Publishers Distributors, 1999
- A.3 R.E. Reed-Hill and R. Abbaschian, *Physical Metallurgy Principles*, 3rd ed., PWS Publishing Company, 1991
- A.4 W.D. Callister, *Fundamentals of Materials Science and Engineering*, 5th ed., John Wiley & Sons, Inc., 2001
- A.5 M. Tisza, *Physical Metallurgy for Engineers*, ASM International, 2001
- A.6 R.M. Brick, A.W. Pense, and R.B. Gordon, *Structure and Properties of Engineering Materials*, 4th ed., McGraw-Hill Book Company, 1977
- A.7 “Determining Average Grain Size,” E112-96, *Annual Book of ASTM Standards*, ASTM International, 1999, p 237–259
- A.8 D.R. Askeland, *The Science and Engineering of Materials*, 2nd ed., PWS-Kent Publishing Co., 1989
- A.9 M. Epler, Structures by Precipitation from Solid Solution, *Metallography and Microstructures*, Vol 9, *ASM Handbook*, ASM International, 2004
- A.10 A.G. Guy, *Elements of Physical Metallurgy*, 2nd ed., Addison-Wesley Publishing Company, 1959

SELECTED REFERENCES

- M.F. Ashby and D.R.H. Jones, *Engineering Materials 1—An Introduction to Their Properties, and Applications*, 2nd ed., Butterworth Heinemann, 1996
- H. Baker, The Chemical Elements, *Metals Handbook Desk Edition*, 2nd ed., ASM International, 1998
- H. Baker, Introduction to Alloy Phase Diagrams, *Alloy Phase Diagrams*, Vol 3, *ASM Handbook*, ASM International, 1992, reprinted in *Desk Handbook: Phase Diagrams for Binary Alloys*, 2nd ed., H. Okamoto, Ed., ASM International, 2010
- T.H. Courtney, Fundamental Structure-Property Relationships, *Engineering Materials, Materials Selection and Design*, Vol 20, *ASM Handbook*, ASM International, 1997
- A.M. Russell and K.L. Lee, *Structure-Property Relationships in Non-ferrous Alloys*, Wiley-Interscience, 2005

- D.R. Sadoway, “The Imperfect Solid State,” Lecture notes, Introduction to Solid-State Chemistry, Department of Materials Science and Engineering, Massachusetts Institute of Technology, Fall 2006
- W.F. Smith, *Principles of Materials Science and Engineering*, McGraw-Hill, 1986

